POLITECNICO
MILANO 1863

SCUOLA DI INGEGNERIA CIVILE,
AMBIENTALE E TERRITORIALE

GROUND PENETRATING RADAR TECHNOLOGY ON THE RAILWAY BALLAST ASSESSMENT

Advisor:
Maurizio Lualdi

Co – Advisor:
Federico Lombardi

MARÍA CAMILA AZCÁRATE NAVARRO

Student number: 963748

Academic Year: 2022 - 2023

ABSTRACT

The ballast layer is the most important component of the railway infrastructure which main function is to redistribute the stresses that come from the track to the ground. This material is constantly exposed to cyclic and heavy loads which may cause change in the particle gradation and, therefore, limitation of its functions. Having said this, the degradation of the ballast layer will influence the performance of the railway track and could potentially lead to derailment with possible disastrous consequences.

In this order of ideas, the ballast layer requires frequent inspection and maintenance. Traditionally, this inspection activity is based on visual evaluation and destructive techniques, as boring tests complemented with laboratory tests. However, those boring test does not provide a continuous information about the subsurface and significant changes on the ground can be neglected.

In recent years, Ground Penetrating Radar (GPR) technology for substructure survey has become more popular, improving to faster systems and better data quality. The GPR is a non-destructive means that can reflect the ballast layer condition by analyzing the received signal variation, creating a continuous profile of the material conditions. This paper reports different laboratory and field studies on GPR application for ballast layer condition evaluation in order to find out which are the features of the ballast material that can be effectively determined by the GPR technology.

At the end it was concluded that the GPR has the ability to detect most of the track substructure problems, being able to detect fouling levels, water trap, layer deformation and layer thickness. Additionally, when combined with other track information, it can provide an excellent tool to make maintenance decisions.

Keywords: railway ballast, Ground Penetrating Radar (GPR), ballast fouling, ballast degradation.

ABSTRACT IN LINGUA ITALIANA

Lo strato di ballast è il componente più importante dell'infrastruttura ferroviaria. La sua funzione principale è quella di ridistribuire al suolo le sollecitazioni che provengono dal binario. Questo materiale è costantemente esposto a carichi ciclici e pesanti che possono causare cambiamenti nella gradazione delle particelle e, quindi, limitazione delle sue funzioni. Detto questo, il degrado dello strato di ballast influenzerà i servizi del binario ferroviario e potrebbe potenzialmente portare al deragliamento con possibili conseguenze disastrose.

Di conseguenza, lo strato di ballast richiede frequenti ispezioni e manutenzioni. Tradizionalmente, questa attività di ispezione si basa sulla valutazione visiva e su tecniche distruttive, come il sondaggio integrato con il test di laboratorio. Tuttavia, i sondaggi non forniscono una informazione continua sul sottosuolo e i cambiamenti significativi sul terreno possono essere trascurati.

Negli ultimi anni, la tecnologia Ground Penetrating Radar (GPR) per l'ispezione delle sottostrutture è diventata più popolare, migliorando a sistemi più veloci con una migliore qualità dei dati. Il GPR è una tecnica non distruttiva che può riflettere la condizione dello strato del ballast analizzando la variazione del segnale ricevuto, creando un profilo continuo delle condizioni del materiale. Questo documento riporta diversi studi di laboratorio e sul campo sull'applicazione del GPR per la valutazione delle condizioni dello strato di ballast al fine di scoprire quali sono le caratteristiche del materiale che possono essere efficacemente determinate dalla tecnologia GPR.

Alla fine, si è concluso che il GPR ha la capacità di rilevare la maggior parte dei problemi della sottostruttura del binario, essendo in grado di rilevare livelli di fouling, presenza d'acqua, deformazione dello strato e spessore dello strato. Inoltre, quando viene combinato con altre informazioni sulla traccia, può fornire uno strumento eccellente per prendere decisioni sulla manutenzione.

Parole chiave: ballast ferroviario, Ground Penetrating Radar (GPR), ballast fouling, degradazione del ballast.

TABLE OF CONTENT

LIST OF FIGURES

LIST OF TABLES

INTRODUCTION

Railways are the most efficient means of transporting goods to the surface of the earth. Additionally, it has a high capacity, efficiency, and low pollution compared to other transportation modes. Over time, the railway's function of connecting residential and production zones has become more critical, enhancing tremendous increases in the technical performance of convoys that, in turn, demand proper support from track-beds. In light of this, a more viable and opportune support is required for railroad ballast to guarantee reasonable security and usefulness conditions at the arranged level. As a matter of fact, the annual investment of founds to construct and maintain a viable track system is enormous (Selig & Waters, 1994).

Ballast is a fundamental component of a track foundation part of the railway system. It provides structural support to the whole system and permits the further distribution and dissipation of the loads over the subgrade. With time, ballast degrades, and its performance becomes limited bringing both economic and safety concerns.

In this order of ideas, the monitoring of the ballast becomes decisive in ensuring an acceptable rail performance acceptable performance of the railway. Presently, the GPR is the leading technique for the assessment of ballast condition, providing a robust assessment of the condition of the track (Li, Hyslip, Sussmann, & Chrismer, 2015).

This document presents a state of art of the GPR technology applied to the evaluation of critical characteristics of the ballast in the railway system. The document is divided in three chapters:

- Chapter one will present a description of the railway system, the definition of the ballast material and description of the ballast profile. Thus, the characteristics, functions and problems of the ballast material are exposed as well as their intervention limits and maintenance techniques.

- The second chapter is dedicated to GPR technology. Starting with a brief introduction about the traditional methods to assess the ballast state. Then it is described in detail the GPR non-invasive technology and their application in the ballast characterization. A section in this chapter is dedicated to the benefits of incorporating the GPR data with other track information. After that

the technology is compared with others survey equipment and at the end, some limitations of the GPR tools are mentioned. All by citing different study cases (laboratory and field studies).

- Finally, in the last part of this document are exposed the conclusions and recommendations for further investigations about the topic.

CHAPTER 1: RAILWAY BALLAST MATERIAL

1.1. DESCRIPTION OF THE RAILWAY SYSTEM

The performance of the railway system depends on the interaction of its components in response to the train loadings. According to Selig & Waters (1994), these components can be grouped in two categories which are the superstructure and substructure as it is presented in the Figure 1 and Figure 2 which schematize a longitudinal and transversal view, respectively, of a typical ballasted track. The superstructure consists of rails, fasteners and sleepers while the last one consists of the ballast, subballast and subgrade.

Superstructure

In the most exposed part of the railway system there are the rails which are the longitudinal steel elements that directly guide the train wheels continuously. These elements must have a sufficient stiffness in order to serve as a beam and at the same time they must transmit the concentrated wheel loads to the sleepers.

Then, below the rail is placed the fastening system which is the connection between the sleepers and the rails. The function of the fastening system is to restrain the rails against the sleepers and resist vertical, lateral, longitudinal, and overturning moments of the rails.

As the last part of the superstructure, there are the sleepers or ties which are elements made mostly of wood and concrete. However concrete sleepers are generally a more secure fasting system than the wood sleeper. One of the main functions of these elements is to transfer the loads from the rails to the ballast and restrain the rail movement. The sleepers usually have a length of 2.5 m, sleeper spacing 0.6 m and cross section 0.26 m x 0.16 m.

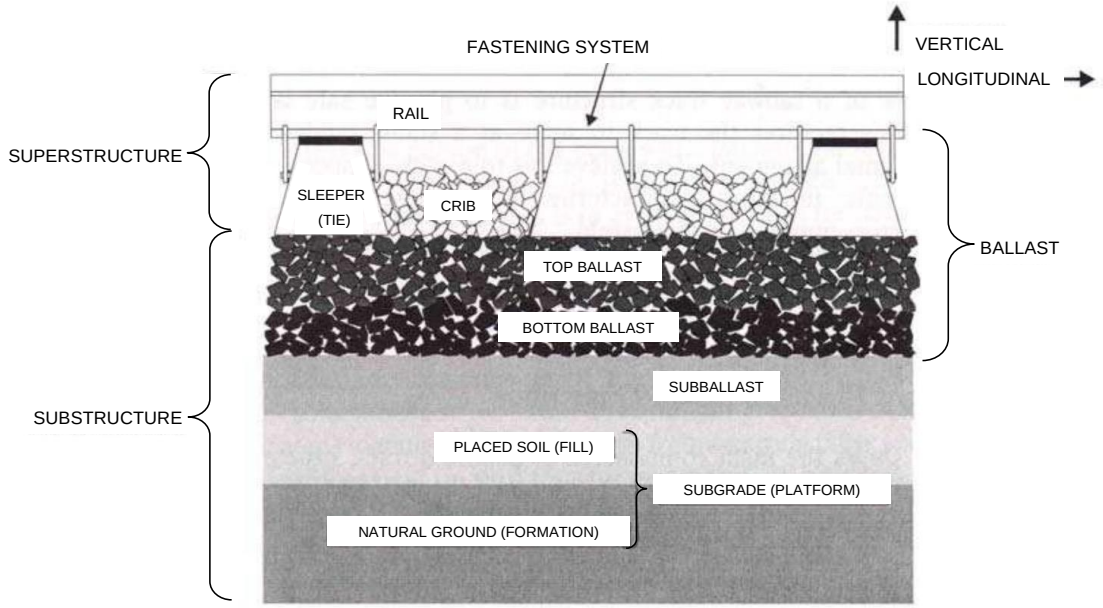

Figure 1. Longitudinal view of the structural component of a typical ballasted track (Selig & Waters, 1994).

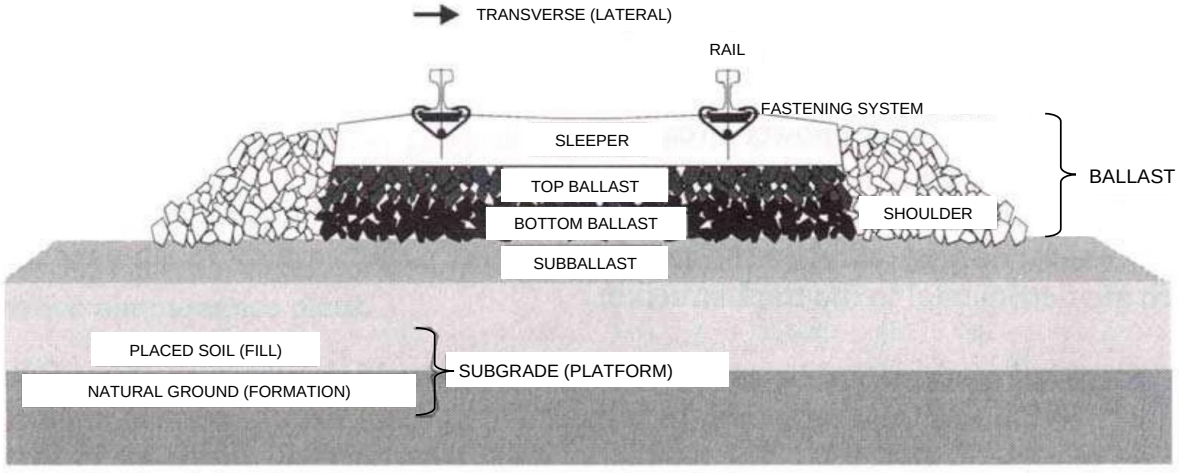

Figure 2. Transversal view of the structural component of a typical ballasted track (Selig & Waters, 1994).

Substructure

In substructure part of the railway system, first there is the ballast layer which is one of the main components of the substructure and is referred to a homogeneously graded hard rock derived material, usually located between, below and around the sleepers with the purpose of ensure lateral stability.

The subballast layer is placed between the ballast and the subgrade layer. It is similar to ballast since it is also a granular material, however this one is finer and broadly - graded than the ballast. Its function is to reduce even more the stress levels on the subgrade and prevent the upward migration of fine material from the subgrade into the ballast. The subballast layer gives a solid support for the top ballast.

Finally, the subgrade is the platform upon which the track structure is built and provides a stable foundation for the subballast and ballast layer. The subgrade can be natural ground or placed soil or fill. The placed fill is used to replace the upper portion of unsuitable existing ground.

It is noteworthy that the substructure contains the components that have the major influence on the cost of track maintenance (Selig & Waters, 1994) because of the variability of its properties which are more difficult to assess compared with the superstructure part.

1.2. DEFINITION OF THE BALLAST

According to the European norm EN 13450/2002 the ballast is defined as: “uniformly graded crushed hard stones, durable, angular and equidimensional in shape, and free from dust, chemical contamination and cohesive particles”. It is usually composed by aggregates with a diameter size ranging between 3 and 6 cm (Bianchini Ciampoli, Calvi, & D’Amico, 2019). According to Selig & Waters (1994), they are "angular, crushed, hard stones and rock uniformly graded, free of dust and dirt, and not prone to cementing actions”. The standard depth of ballast is 0.3 m (RailCorp, 2015), however, this thickness value can vary depending on the operation classes.

Almost all the important railway tracks are provided with broken stone ballast that should be hard, tough and nonporous (The constructor, 2019). This material is obtained by crushing hard stones like granite and limestones (see Figure 3), it is suitable for heavy traffic tracks and for high-speed tracks. One of it befits it is that the broken stones are hard and durable, they hold the sleepers in a strong position, which provides stability to the track, and they require less maintenance compared to other materials. Nonetheless, this type of material is not easily available, and their initial cost can be higher compared with other types of ballast as is the gravel ballast. Moreover, the broken stones ballast are sharp and angular elements, therefore, wooden sleepers may be liable to damage by these broken stones.

Another material used as ballast is gravel as it can be seen in the Figure 3. This is a naturally occurring material that comes from the erosion of the rocks. The advantage is that, since it occurs naturally, it is cheap and easily available. However, this material must be properly cleaned, otherwise the drainage properties of gravel may be affected. When the gravel ballast is well packed, it will require less maintenance during its lifetime, beside has a high durability. One important drawback of this material is the fact that they may get separated from the bed under vibrations because of their smoothness and roundness.

Figure 3. From left to right in the first row: Granite, Basalt and Limestone. From left to right in the second row: Slag and Gravel. (The constructor, 2019).

Finally, coal ash can be also used as ballast material (see Figure 4). They are the product of coal fired plants and railway locomotives. The coal ash can be used as a ballast material, especially for station yards, since it possesses good drainage properties. The advantages of this material with respect to the others are that it is economical and abundantly available. Also, it can be handled with ease since it is light in weight. The problem is that this type of ballast can be turned into dust when subjected to loads, making the track dirty and complicating the maintenance procedure. Additionally, the rails may get affected by the corrosive action of coal ash.

Figure 4. Coal ash ballast. (The constructor, 2019).

1.3. BALLAST PROFILE

In the next figure is presented a typical ballast profile where is show the different positions of the material in the railway.

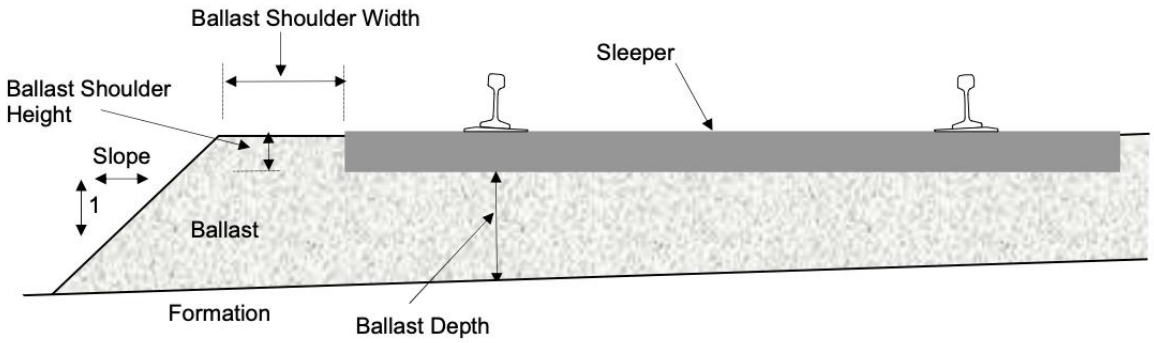

Figure 5. Typical track cross-section and ballast profile (RailCorp, 2015)

First there is the ballast shoulder, which is the material placed around the sleeper's end. Their function is to provide lateral stability to the track. The width for the ballast shoulder typically ranges between 300 – 600 mm with a slope of 1:1.5 (height : width).

Then, the crib, which is the loose ballast that is between the sleepers, has the function to lock the sleepers and the rail in place. The crib height should be 5 cm lower than the sleeper's top surface.

Finally, the ballast depth is defined as the distance from the underside of the sleeper to the top of the finished formation. The depth of the ballast section is an important factor since the load carrying capacity and distribution of traffic load depends on it. The deeper the thickness of the ballast layer, the higher will be the load-carrying capacity of the track. The RailCorp (2015) which regulates the railway transport in new south Wales, Australia, defines 3 ballast depth categories: high, medium or low and for each of them is define a range value as is presented in the Table 1. Then, the Table 2 shows different operation classes and the corresponding ballast depth.

Category		Design Ballast depth(mm)	
		Minimum	Maximum
High	H	350	500
Medium	M	300	500
Low	L	250	500
	L(150)	150	500
	L(100)	100	500
	L(Nom)	Nominal	500

Table 1. Ballast Depth categories.

Operating Class	New		Existing	
	Sleeper type	Ballast depth (Note 3)	Sleeper type	Ballast depth (Note 1, 2)
Main line				
Passenger Main Line	Medium duty concrete	L	Timber	L
	Heavy duty concrete			
Mixed Passenger Freight Main Line	Medium duty concrete	M	Timber	M
	Heavy duty concrete			
Light Line	NA		Timber	L
Heavy Freight Option	Heavy duty concrete	H	Heavy duty concrete	H
Sidings				
General Yard(1)	Medium duty concrete	L	Timber	L(150)
Passenger operations/ or maintenance	Medium duty concrete	L	Timber	L(150)
Passenger Siding	Timber	L(100)	Timber	L(100)
Engineering Maintenance Siding	Timber	L(Nom)	Timber	L(Nom)

Table 2. Ballast height.

Similarly, Selig & Waters (1994) propose different ballast depth depending on the function defining that a minimum between 300mm and 450mm ballast is required below the sleepers and this applies to heavily used track.

It is important to remark that an insufficient depth of ballast will overload the underlying subgrade. In the worst cases, this can cause track deformation and affect the ride and operation of the trains.

1.4. BALLAST SPECIFICATIONS

Depending on the country, the specifications of the ballast may change, therefore, there is not a universal definition of the requirements that the ballast sublayer of the railway demand. However, the criterium used to characterize the ballast may coincide among the normative. Here is presented the Australian rail track corporation (ARTC) and the Rete Ferroviaria Italiana (RFI).

Before presenting the specification from each normative, the definition and methodology for the test used to characterize the ballast material is given.

- The content of fine particles must be determined, as indicated by the UNI EN 933-1 standard, by sieving through a 0,063 mm sieve the material resulting from the washing of a representative sample weighing not less than 60 kg.

- Bulk density is calculated as the mass of the soil sample per unit volume including voids, or the weight of the soil sample for a given volume. This is according to the AS 1141.4 for the ARTC normative.

- Particle density is estimated according to the AS 1141.6 for the ARTC and UNI EN 1097-6 for the RFI. Is the mass of a soil sample in each volume of particles (mass divided by volume). Particle density is focused only on the soil particles and not the total volume that the soil particles and pore spaces occupy in the soil. The particle density differs from bulk density because this last one includes the volume of the solid portion of the soil along with the spaces where air and water are found.

To characterize the shape of the ballast aggregate it is mentioning the flakiness index test and the crushed particles percentage.

- According to the ARTC, the flakiness Index of aggregate is the percentage by weight of aggregate particles whose least dimension is less than 0.6 of their mean dimensions. The flakiness Index it is estimated according to the AS 1141.15 as the weight of flaky particles in the ballast material retained on the 6.70 mm expressed as a percentage of the total weight of the sample gauged. While for the RFI normative, the test is named shape coefficient and the criterium is similar to the flakiness index. As indicated by the UNI EN 933-4, the shape coefficient must be determined in a sample not less than 40 kg and

is the percentage by weight of the elements having the minimum dimension less than 1/3 of the maximum.

- Crushed particles of coarse aggregate of the ballast material are determined in accordance with AS1141.21. This requirement has the purpose of maximizing shear strength by increasing inter-particle friction. The test procedure is based mostly on visual inspection. First the sample is weight and then is spread on a clean flat surface. After that, by visual inspection it is separate uncrushed particles from crushed particles and the crushed particles are weighed.

To test the durability of the ballast it is going to be mentioned three tests: Aggregate crushing value, wet attrition value and the resistance to ice and thaw cycles

- The aggregate crushing value is determined in accordance with AS1141.21. The aim of this test is to obtain produced fines by crushing. The procedure consists in taking a measured quantity of sized aggregates and submit them to a force of 400kN within a confined space. Then the fraction of material passing the 26.5 mm test sieve and retained on 19.0 mm test sieve shall be measured. Aggregates with lower crushing value show a lower crushed fraction under load and would give a longer service life to the road.

- The wet attrition value is determined in accordance with AS1141.27. The test instrument is the Deval attrition apparatus that has a container in which the sample is rotated for 10.000 rotations. Then the sample of the material passing the 53.0 mm test sieve and retained on 37.5 mm test sieve shall be measured.

- The RFI use the resistance to ice and thaw cycles according with the UNI EN 1367-1. The percent loss of resistance is calculated according to the following equation (Eq. 1).

$$\Delta S_{LA} = \frac{S_{LAi} - S_{LA0}}{S_{LA0}} \; x \; 100 \qquad \textit{Eq. 1}$$

Where:
ΔS_{LA} = percentual loss of resistance
S_{LA0} = Los Angeles coefficient of the sample before the ice and thaw cycle

S_{LAi} = Los Angeles coefficient of the sample after the ice and thaw cycle

To measure the fragmentation resistance, it is use the Los Angeles test and the weak particles estimation.

- Los Angeles values is determined in accordance with AS1141.23 for the ARTC and UNI EN 1097-2 for the RFI. This test measures the resistance of ballast to fragmentation by providing a Los Angeles Abrasion (LAA) coefficient. The definition of the LAA is the percentage of the test portion passing a 1.6mm sieve after the completion of the test. So, ballast specimens with high values of LAA are more susceptible to fragmentation (Lim, 2004). The test is performed in a steel rotation drum loaded with 12 spherical steel balls weighing approximately 5.2 kilograms. The drum is rotated for 500 revolutions and fine particles are generated in this process. After that the sample is sieved and the percentage loss of the samples is the LA abrasion loss as is presented in the next equation (Eq. 2).

$$LA_{RB} = \frac{Pi - m}{Pi} x100 \qquad \textit{Eq. 2}$$

Where:
Pi = initial mass of the sample in gr
m = retained mass in the 1.6 mm sieve in gr

- Weak particles are determined in accordance with the AS 1141.32. This test is used to evaluate the cleanliness of the aggregate through the percentage of weak particles, that is the particles that will deform under finger pressures when wet.

Characteristic	Test	ARTC	RFI
Fine particles	Fine particles	-	0.5% max
Density	Bulk density	> 1200 kg/m^3	-
	Particle density	> 2500 kg/m^3	> 2310 kg/m^3
Shape	Flakiness index	30% max	20% max
	Crushed particles of coarse aggregate	95% min	-
Durability	Aggregate crushing value	25% max	-
	Wet attrition value	6% max	-
	Resistance due to ice and thaw cycles	-	20% max
Fragmentation resistance	Los Angeles value	25% max	26% max
	Weak particles	5% max	-

Table 3. Comparative table of the specification of the railway ballast.

Finally, the dimensional requirements must be assessed through the granulometric analysis performed according to the UNI EN 933-1 standard for the RFI and AS 1141.11 and AS 1141.12 according to the ARTC. This test is carried out by sieving, where an aggregate sample is shaken through a selected sieve sizes from largest down to smallest. The result is reported as the percentage passing each individual sieve size. The Table 3 present the characteristics of the material and the test used to characterize it, likewise the limit or recommended value of each test of each of the normative. Additionally, the dimensional requirements of the material according to the ARTC and the RFI are presented in the Table 4 and Figure 6 respectively.

It can be noticed that the limits values for the test criterium that the normative has in common, are relatively the same. Similarly, by analyzing the granulometric requirements it is evident that the limits are very similar.

Sieve Size (mm)	Nominal Size (mm)
	60
	% passing by mass
63.0	100
53.0	85-100
37.5	20-65
26.5	0-20
19.0	0-5
13.2	0-2
9.50	-
4.75	0-1
1.18	-
0.075	0-1

Table 4. Granulometric limit (ARTC A. , 2007)

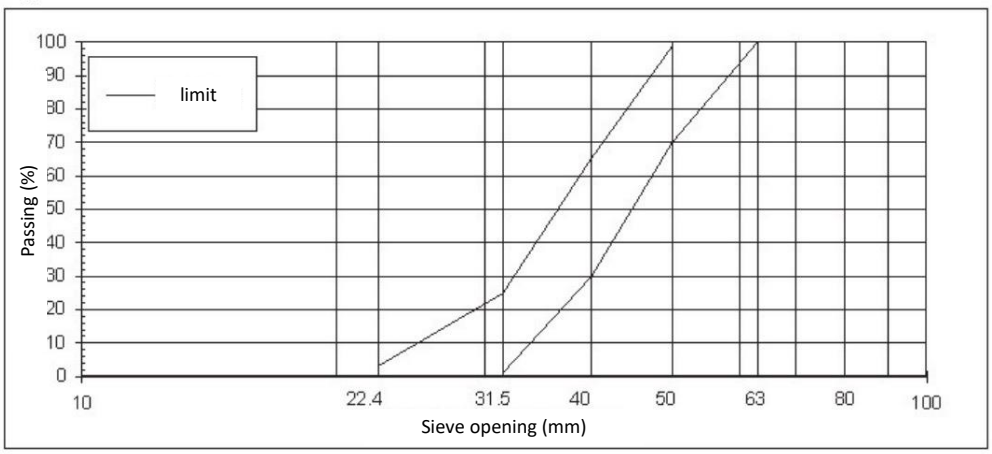

Sieve opening	mm	80	63	50	40	31.5	22.4
Passing	%	100	100	70÷99	30÷65	1÷25	0÷3

Figure 6. Granulometric limit (Rete Ferroviaria Italiana RFI , 2020)

1.5. BALLAST FUNCTIONS

Ballast has many functions for the railway system. According to Selig & Waters (1994) the most important are:

- Restrains the track laterally, longitudinally, and vertically under dynamic loads imposed by trains and thermal stress. The vertical forces come from the wheel (see Figure 7) while the longitudinal forces come from the locomotive traction force when braking, these occur along the rails. The lateral forces are the one that are constrained by rail/fastening, fastening/sleeper, and sleeper/ballast interaction.

  In term of forces, generally each cars loading has 4 axles, each of them generating 200 kN vertically and 45 kN longitudinally (Esveld, 1998).

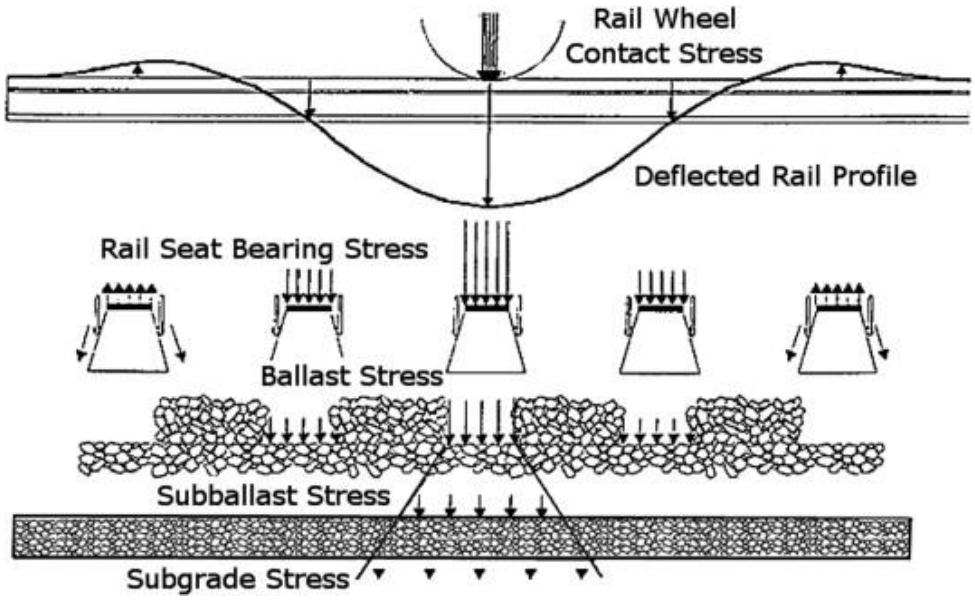

Figure 7. Vertical forces acting on the railway track. (Selig & Waters, 1994).

- Distributes the load of the track and train to prevent over stressing the subgrade and possible rail deflection, temporary or permanent. Stress distribution is presented in Figure 8 proposed by Esveld (1998).

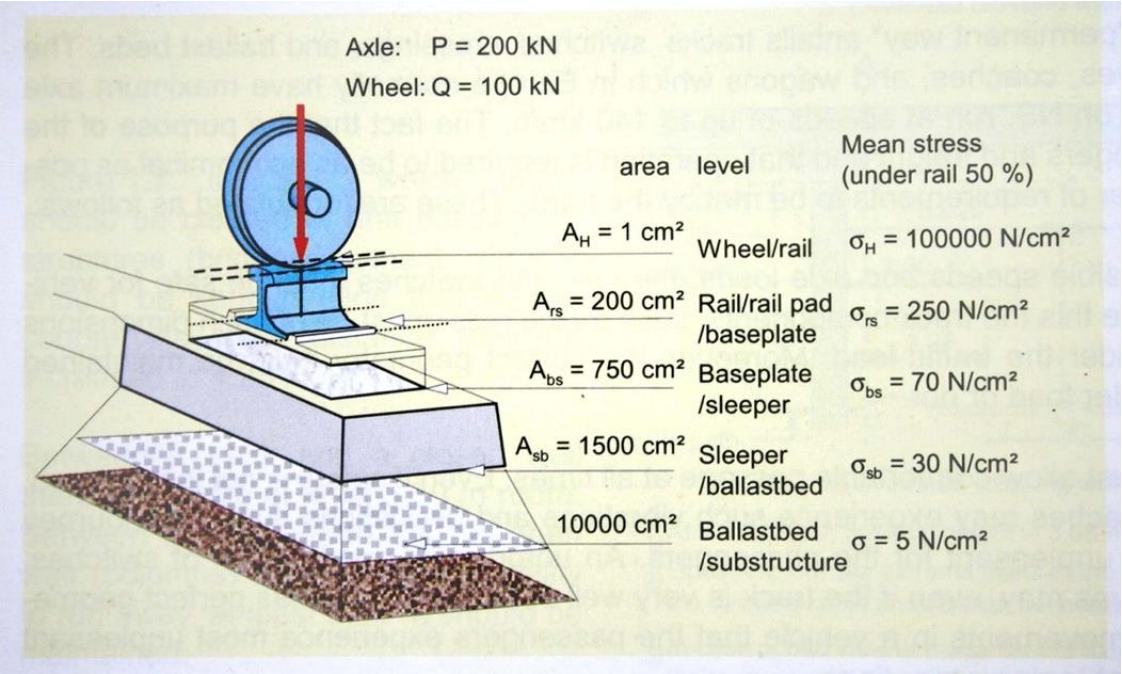

Figure 8. Stress distribution on the railway. (Esveld, 1998).

In the previous figure it can be notice the reduction in stress from 30 N/cm^2 at sleeper-ballast bed interface to 5 N/cm^2 at ballast bed-formation interface.

According with Esveld (1998), the equivalent ballast resistance at 1 meter of track is equal to 500 N/cm^2 in both longitudinal and lateral direction. Additionally, the typical value of longitudinal resistance for concrete sleepers in ballast is 11 kN/sleepers.

- Provide resilience and energy absorption to the track which reduces the stresses in the underlying materials to tolerable level.

- Provides adequate drainage of the water falling onto the track. The water should not stay neat the track since this will compromise the ground that supports the railway track system. Besides providing drainage for the water

falling onto the track, the ballast also stores fouling materials due to its large voids.

- Maintains proper track levelling and alignment. The ballast facilitates the maintenance operations due to the ability to rearrange ballast particles in the tamping process.

- Retards growth of vegetation that might interfere with the track.

- Provides electrical resistance between rails.

- Attenuation of noise and vibration generated by the load of the trainsets.

1.6. BALLAST PROBLEMS

Over the lifetime of the railway structure, the ballast progressively deteriorates bringing repercussions in the railway system such as change in the ballast track geometry, risk of derailment, differential track settlement. Regarding the substructure, it was emphasized that fouling is one of the primary causes of failure and an early detection may be crucial to reduce future costs of intervention (Artagan, Bianchini Ciampoli, D'Amico, Calvi, & Tosti, 2019). Fouling refers to the condition of railroad ballast layer when voids in unbound aggregate layer are filled with relatively finer materials or fouling agents commonly generated by ballast aggregate breakage, outside contamination such as coal dust from coal trains, or from subgrade soil intrusion (Moaveni, Qian, Boler, Mishra, & Tutumler, 2014).

The Figure 9 represent graphically three phases of ballast contamination conditions, from clean ballast to heavily fouled ballast.

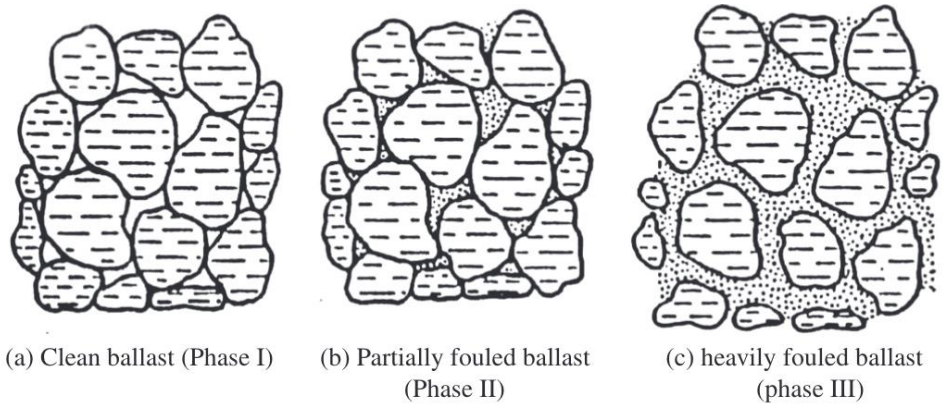

Figure 9. Ballast fouling phases. (Tutumluer & Huang, 2011)

The phase I shows a clean ballast with almost all aggregates in contact with each other. Then in the phase II, the voids are filled with fine particles which can significantly reduce the strength in the ballast aggregate layer. Finally, the phase III presents a fouled ballast condition where almost all the contact between the aggregates are eliminated. The fouled ballast condition causes a decrease in the permeability which means delay in dissipation of excess pore water pressures. This will affect the mechanical resistance of the material.

Ballast fouling, often associated with deteriorating railroad track performance, refers to the condition when the ballast layer changes its composition and becomes much finer in grain size distribution (Moaveni, Qian, Boler, Mishra, & Tutumler, 2014).

According to Selig & Waters (1994), there exist different sources of fouling and the most important one fines from ballast abrasion and small particles from ballast breakage (76%). With a less percentage as a source of ballast fouling are the migration upward of underlying granular layer (13%), fines form the subgrade (3%) due to seepage forces, inclusion of fines from the surface (7%) due to wind or water transported, and sleeper wearing (1%). The percentage of participation of each source was proposed by Selig & Waters (1994) as is presented in the Figure 10.

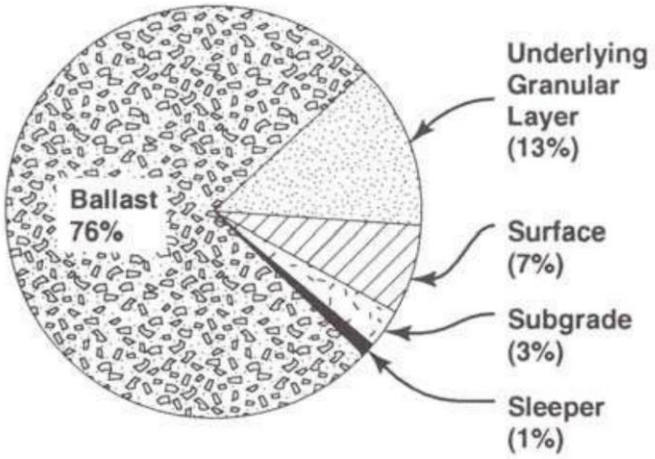

Figure 10. Sources of ballast fouling (Selig & Waters, 1994).

According to Bassey et alt. (2020) ballast fragmentation accounts for a significant fraction of commonly recorded contaminations, especially in the United States, while on the contrary, in the United Kingdom, mostly in the coal transportation line, the main source of fouling observed is surface weathering and in a second place, the ballast fragmentation. Nevertheless, ballast degradation is still the main fouling source (Wang, et al., 2022).

The breakage of the ballast could happen due to the characteristics of the ballast parent rock (e.g., hardness, specific gravity, grain size, toughness, weathering, mineralogical composition, etc.) and/or field factors (e.g., presence of water, confining pressure, thickness of the ballast layer, dynamic loading pattern, etc.) (Li, Hyslip, Sussmann, & Chrismer, 2015). The ballast particles also deteriorate rapidly during tamping process (Wang, et al., 2022). Tamping breaks and wears ballast particles. As a matter of fact, Tutumluer et al., (2006) proved that ballast tamping reduces significantly the shear resistance of angular aggregates up to 40%. In addition to that, after the tamping process, there is a drop in the lateral resistance to about 30% to 70% with respect of the initial condition (Jing & Aela, 2020).

Other sources of fouling are the infiltration from outside of ballast layer and the main contribution of this source comes from the underlying granular layer causing ballast pockets (Selig & Waters, 1994). The ballast pockets inevitably occur because under cyclic loading and ballast weight, the ballast and subgrade intrude into each other. The ballast pockets may give place to mud pumping, which is typically caused by huge amount of rainfall storage that occurs in those ballast pockets. Mud pumping is the process by which water and fouling are drawn up to the surface of the ballast layer.

It is imperative to point out that, when fouling reaches important levels, the structural integrity and draining capacity of the contaminated ballast can be compromised (Calvi, Cutolo, Bianchini Ciampoli, & Brancadoro , 2016). This can be evidence in the Table 5 proposed by Selig, E.T., et alt (1993), where is show the hydraulic conductivity for different fouling categories. This may lead to instability of the superstructure which, as a last consequence, may lead to derailment of the trainsets and excessive lateral move.

Fouling Category	Fouling Index	Hydraulic Conductivity, k_h	
		(in./sec)	(mm/sec)
Clean	<1	1-2	25-50
Moderately clean	1-9	0.1-1	2.5-25
Moderately fouled	10-19	0.06-0.1	1.5-2.5
Fouled	20-39	0.0002-0.06	0.005-1.5
Highly fouled	>39	<0.0002	<0.005

Table 5. Hydraulic conductivity values for ballast at different fouling conditions. (Selig, Parsons, & Cole, 1993).

The fouling can also bring consequences in terms of settlements. As we can see in the Figure 11, the fouled track portion will accumulate more settlement than the clean track and this may lead to a “hanging tie” scenario.

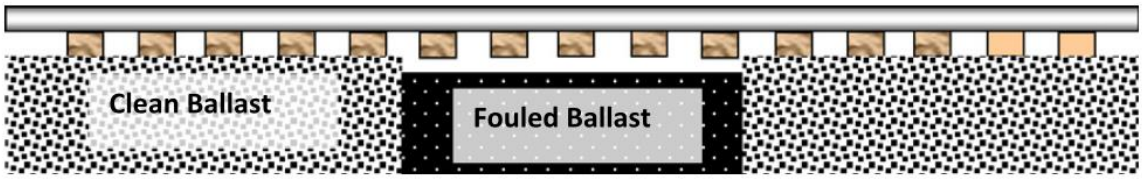

Figure 11. Hanging tie scenario due to ballast fouling. (Tutumluer & Huang, 2011)

The same hanging tie scenario might occur due to the tamping process itself. Tutumluer et al., (2006) investigated the effect of the tamping in ballast behavior. The results are illustrated in the Figure 12.

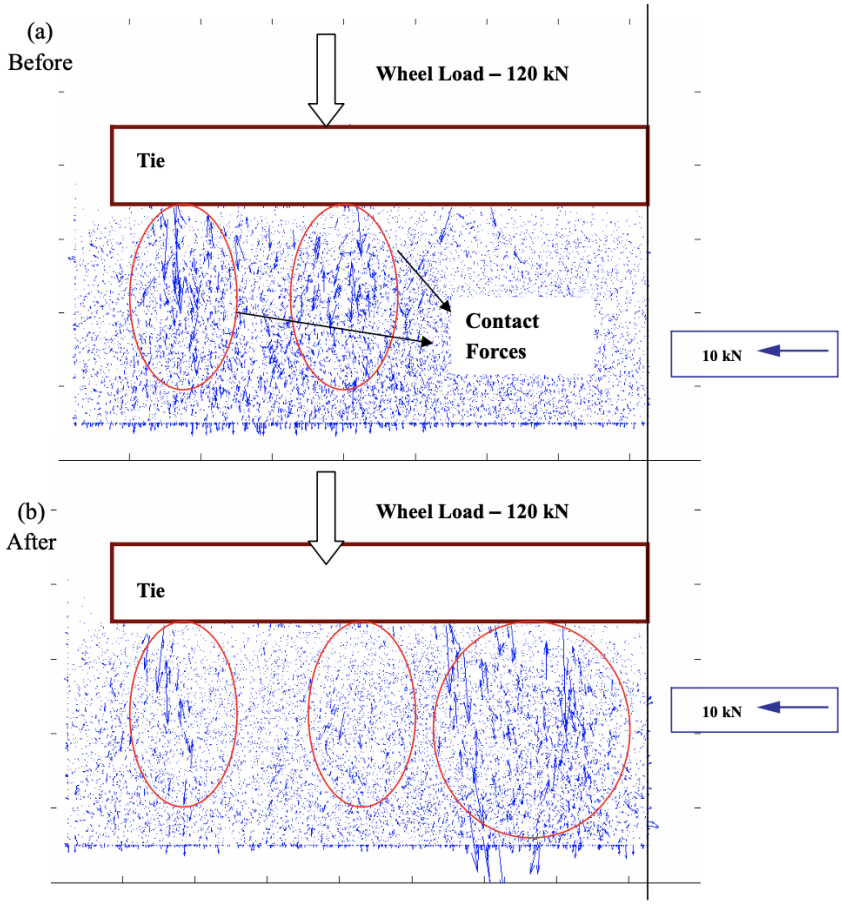

Figure 12. Aggregate Contact Forces Predicted in the Ballast Before and After Tamping. (Tutumluer E. , Huang, Hashash, & Ghaboussi, 2006).

Tutumluer et al., (2006) conclude that initially, there is a great amount of contact forces provided by the ballast particles immediately under the wheel loading position. However, during and after tamping, these particles are disturbed to transform into a

looser state and the major contact forces are moved to the center of the tie. This phenomenon is referend to as the center bound tie which can considerably decrease the tie service life.

Among other consequences, the fouling affects the elasticity of the ballast which difficult the maintenance activity as tamping/packing and reduce its ability to dissipates the dynamic loads (Wang, et al., 2022). The ballast layer hardens when the fouling fills the voids between ballast particles, therefore, the stiffness of ballast layer increases, and resilience reduces (Sadeghi, Motieyan-Najar, Zakeri, Yousefi, & Mollazadeh, 2018).

As a remedial measure for the fouling problem in the ballast, preventive maintenance such as ballast cleaning can be implemented in order to ensure extended life for the ballast. These techniques are going to be explained in further sections.

The fouling level (or fouling rate) is very hard to observe from the ballast layer surface or to judge from the dynamic responses until mud pumping and serious ride comfort occur (Wang, et al., 2022). In other words, the problem of fouling content in the ballast layer of the railway track system requires deep inspection techniques in order to be assessed with enough time to take remedial actions.

Usually, to predict the fouling it is used the typical drilling and sampling process taken at some part of the railway track, which means that the measurements are not continue nor accurate. In the other hand, the use of non-destructive techniques, as is the GPR, can provide a continuous survey with less time and effort. This technology is going to be developed in subsequent chapters.

1.7. INTERVENTION LIMITS OF THE BALLAST

The bearing capacity of the substructure is an important issue for designers and maintainers as differential settlements are usually reported to occur in the substructure part of the railway system (Li, Hyslip, Sussmann, & Chrismer, 2015). This can affect the safe ride and the normal operation of the trains. Problems in the ballast layer, as mentioned in the previous section, occur mainly because of the fouling which main source is the ballast that breaks under the cyclic and heavy traffic loads. In this order of ideas, the intervention limits of the ballast can be analyzed in terms of ballast gradation limits with the breakage index and fouling limits with the fouling index.

Ballast gradation limits

The grain size distribution of ballast is the most common specification for the assessment of ballast since it allows reliable correlation to strength, deformation, and drainage characteristics (Bassey, Ngene, Akinwumi, Akplan, & Bamigboye, 2020). According to the specifications and norms like the European norm EN 13450/2002 and RailCorp (2015), the ballast requires a relatively narrow range of particle sizes which maximizes interparticle void volume that will facilitate drainage and provides storage for ballast fouling material. This is evidence in the Figure 13 where is presented typical ballast gradation around the world, in particular the grain distribution used in Australia (Queensland and RIC which is the Rail Infrastructure Corporation NSW), in France, and in the US (AREMA which is the American Railway Engineering and Maintenance-of-Way Association) being the AREMA No. 24 with a field void radio typically of 0.5 the most adopted gradation in the US. There are different gradation and ballast specifications around the world, therefore, there is not a universal definition of the requirement of the specification on this material, it will depend on the country.

The ballast fragmentation primarily refers to all deformations away from the originally recommended gradation of the ballast (Bassey, Ngene, Akinwumi, Akplan, & Bamigboye, 2020). Therefore, in order to evaluate track ballast fragmentation, the breakage index is implemented which is obtained as the summation of the extra mass retained on each sieve during the deterioration and fragmentation of the ballast. Higher fines content represents a higher degree of fouling, therefore, a more graded particle size distribution in the material.

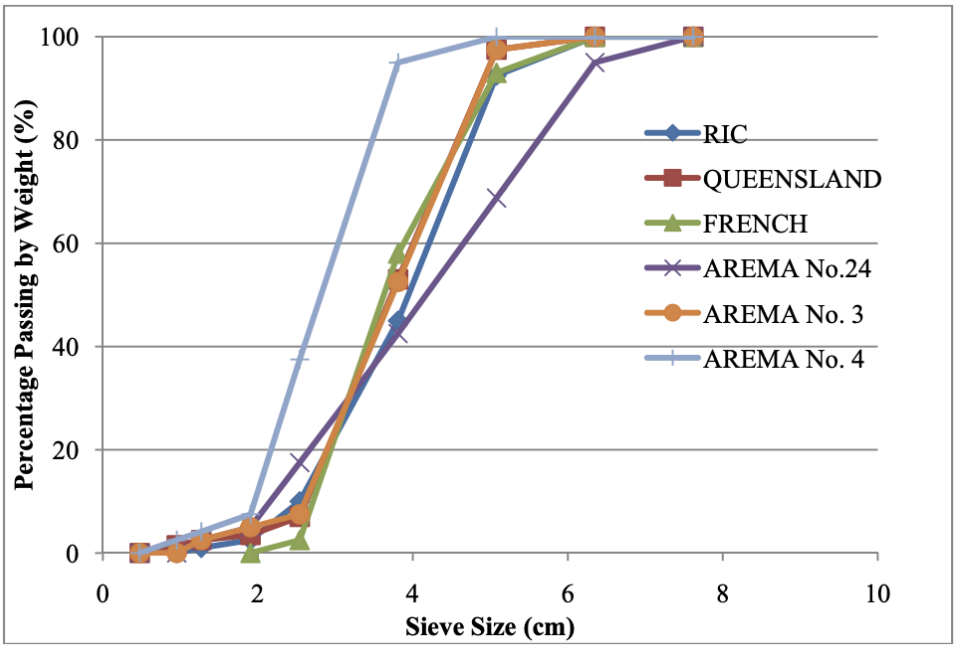

Figure 13. Common ballast gradation (Tutumluer E. , Huang, Hashash, & Ghaboussi, 2009).

Ballast fouling limits

As it was mentioned previously, the fouling in the ballast leads to significant drainage problems, differential settlements, and it increased the track maintenance frequency. The follow table proposed by Li, D. et al., (2015) compares several ballast fouling intervention levels. The two main criteria used to assess the fouling content are the fouling index (for Selig & Waters and Spoornet) and a single sieve size percent passing criteria (for Ruel, UIC and ERRI).

Agency or source	*Criteria/size mm (in.)*	*Limit (%)*	*Rationale for intervention*
Selig and Waters	Fouling index (FI)	40	Highly fouled
		30	Drainage reduction
Spoornet	$FI_{Spoornet}$	80	Gradation change
Canadian National (Ruel)	19 mm (3/4 in.)	40	Highly fouled
UIC	14 mm (1/2 in.)	30	N/A
ERRI	22.4 mm (7/8 in.)	30	N/A

Table 6. Ballast fouling intervention level comparison (Li, Hyslip, Sussmann, & Chrismer, 2015).

The first criterium in the table is the one proposed by Selig and Waters (1994). They define the fouling index (FI) as follows (Eq. 3).

$$FI = P_4 + P_{200} \quad \textit{Eq. 3}$$

Where P_4 is the percent passing the #4 sieve (4.76 mm) and P_{200} is the percentage passing the #200 sieve (0.074 mm).

It is important to point out that with this formula the material passing the 0.075 mm sieve is counted twice. This is to accentuate the effect of the finer material due to its very large influence on permeability and, therefore, with draining properties of the ballast. Additionally, Selig and Waters (1994) also defined four categories of fouling (clean, moderately clean, moderately fouled, fouled, and highly fouled) based on the FI as is presented in Table 7.

Category	Fouling index (Selig and Waters 1994) (%)	Percentage of fouling (%)	Relative ballast fouling ratio (%)
Clean	<1	<2	<2
Moderately clean	1 to <10	2 to <9.5	2 to <10
Moderately fouled	10 to <20	9.5 to <17.5	10 to <20
Fouled	20 to <40	17.5 to <34	20 to <50
Highly fouled	≥40	≥34	≥50

Table 7. Categories of fouling based on the fouling index, percentage of fouling, and relative ballast fouling ratio. (Selig & Waters, 1994).

Based on the criterium of Selig and Waters (1994) it is set as a limit of contamination 40%, which means that, at this level, the ballast shall be considered to have failed to meet functional requirements.

The second criterium presented in the Table 6 was proposed by South African Railway Spoornet (Vorster, 2012). This is an alternative FI based on the percent passing the 19 mm, 6.7 mm, 1.18 mm, and 0.15 mm sieve. The formulation of the FI is presented in Eq. 4.

$$FI_{spoornet} = 0.4P_{19} + 0.3P_{6.7} + 0.2P_{1.18} + 0.1P_{0.15} \quad \textit{Eq. 4}$$

Where:

$$P_{0.15} = \frac{(\%\ by\ mass\ of\ material\ finer\ than\ the\ 0.15\ mm\ sieve) \times 100}{27} \quad \textit{Eq. 5}$$

$$P_{1.18} = \frac{(\%\ by\ mass\ of\ material\ finer\ than\ the\ 1.18\ mm\ sieve) \times 100}{11.5} \quad \textit{Eq. 6}$$

$$P_{6.7} = \frac{(\%\ by\ mass\ of\ material\ finer\ than\ the\ 6.7\ mm\ sieve) \times 100}{18} \quad \textit{Eq. 7}$$

$$P_{19} = \frac{(\%\ by\ mass\ of\ material\ finer\ than\ the\ 19\ mm\ sieve) \times 100}{27} \quad \textit{Eq. 8}$$

Based on this definition of the FI, Spoornet (Vorster, 2012) defines a cleaning limit when FI reaches 80%. The reason for the difference between the intervention limits of Spoornet and Selig & Waters is the sieves that they consider in their estimation of the FI.

The last three criterium in the Table 6 are simpler approaches based on the percentage of material passing a single-sieve size. The Canadian National criterium, which is also use in United States, consider the percentage of material passing the ¾ inch (19 mm) sieve. With this approach it is set as a limit of undercutting maintenance limit 25 to 35%, while 40% is considered the ballast life limit. Similarly, the UIC (International Union of Railways) define the criterium as the mass finer than the 14 mm sieve and the limit for intervention is 30% while the European Rail Research Institute (ERRI) is the mass finer than the 22.4 mm rectangular sieve and the limit is set at 30%.

In the other hand, in some cases it is more convenient to use a different indicator of contaminants in the ballast layer. This is the percentage of void contamination (PVC) which is defines as the Eq. 9 (Tennakoon, Indraratna, Rujikiatkamjorn, Nimbalkar, & & Neville, 2012):

$$PVC = \frac{V_2}{V_1} \times 100 \quad \textit{Eq. 9}$$

Where V_2 is the volume of contaminates and V_1 is the volume of voids within the ballast profile in a compacted state.

The difference between FI and PVC is that the first one is a weight measure of fouling while the last one is in term of voids. The FI method turns out to be inappropriate to use for coal railway due to the low specific gravity of the fouling material (the coal). In this order of ideas, an equal mass of coal can be contained in twice the volume of either granite or clay (Bassey, Ngene, Akinwumi, Akplan, & Bamigboye, 2020). Therefore, only when the fouling material is of a similar specific gravity than the ballast material, a PVC index turn to be similar to a FI.

The Aurizon network, which owns and manages the central Queensland coal network, defines its intervention level with the values of PVC setting a maximum of 30% (AURIZON, 2015). This limit is also supported by North America, South Africa and Europe. In particular in Europe, as it was mentioned above in the Table 6, the ERRI limit is set at 30%, although it considers a weight measure of fouling. Similarly, in North America the ballast contains more than 30% of fines sized less than 22 mm sieve then ballast cleaning becomes appropriate, if there is more than 40 %, then ballast cleaning is inevitable (Guidelines to the Best Practice for Heavy Haul Railway Operations, 2009). Notice that here it compares two indicators of contaminants FI and PVC.

Finally, the Figure 14 proposed by Selig & Waters (1994) presents the impacts of contaminants on the reduction of drainage capacity of the ballast. It can be noticed that by increasing the quantities of contaminants in the void spaces, the permeability is highly limited therefore it produces the retention of water in the ballast layer. The limit point at which ballast drainage capacity becomes significantly impeded by fouling agents is an FI = 30 where the surface water drainage rate is less than 1 mm/hr.

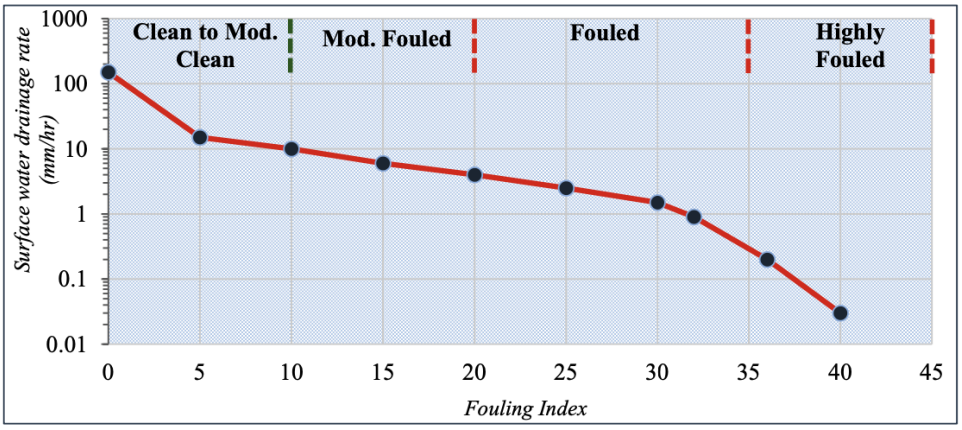

Figure 14. Surface water drainage rate and FI relationship (Mod = moderately) (Selig & Waters, 1994)

1.8. MAINTENANCE TECHNIQUES

The deterioration of the railway track system throughout time is a condition that needs to be constantly monitored. The end of ballast life usually coincides with the voids being filled with fouling material, which reduces the permeability to the point that the drainage function is lost (Li, Hyslip, Sussmann, & Chrismer, 2015). Track maintenance is needed to guarantee the railway track operation. The main track maintenance operations are described in the follow paragraphs.

Tamping

The basic principle consists in moving the ballast particles through the vibration and squeezing the tamping tines when lifting the track. The typical tamping machine it is show in the next figure.

Figure 15. Tamping machine. (The constructor, 2019).

The entire tamping process is divided into four stages as is presented in Figure 16 (Guo, Markine, & Jing, 2021). First the track is lifted 20 mm then the tamping tines penetrate the ballast bed with a certain oscillation frequency. Afterwards the tamping tines squeeze to move crib ballast particles to the locations under sleepers, and finally the tamping tines are lifted, and the tamping machine moves to the next sleeper to repeat the tamping process.

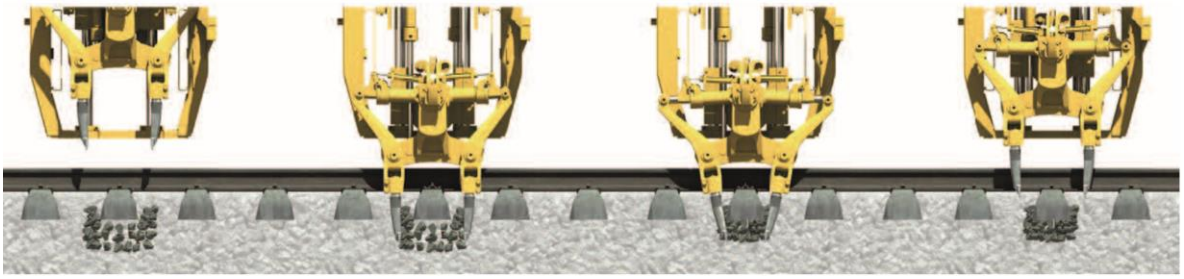

Figure 16. Stage of the tamping process. (Guo, Markine, & Jing, 2021)

However, there are some negative effects in the ballast material after the tamping process as is the drops in the lateral resistance to about 30–70% of the initial condition (before tamping) (Jing & Aela, 2020). A solution to this reduction of resistance in the material after the tamping process is to implement a track stabilizer after tamping to quickly compact the ballast layer (Guo, Markine, & Jing, 2021). Jing & Aela (2020) also affirm that the dynamic track stabilization restores 30–50% of resistance.

Stone blowing

The stone blowing process is an alternative to tamping. Stone blowing uses this same concept to correct track profile error, except that instead of being placed by shovel, the stone is blown into the void between tie bottom and ballast bed using pneumatic injector tubes that are driven into the ballast along the side of the raised tie (Li, Hyslip, Sussmann, & Chrismer, 2015). This process is illustrated in the Figure 17. It can be notice that, different from the tamping process where the existing ballast packing condition is disturbed, here the ballast is injected.

A design is used to determine how much stone should be blown in to achieve the desired rail elevation. A measured amount of stone is blown under the raised tie after compressed air is applied to the tubes, which have been inserted into the ballast to a depth that gives the stones a flow path and access beneath the tie. The procedure is then repeated with the removal of the stone blowing tubes and their placement along the side of the following raised tie (Li, Hyslip, Sussmann, & Chrismer, 2015).

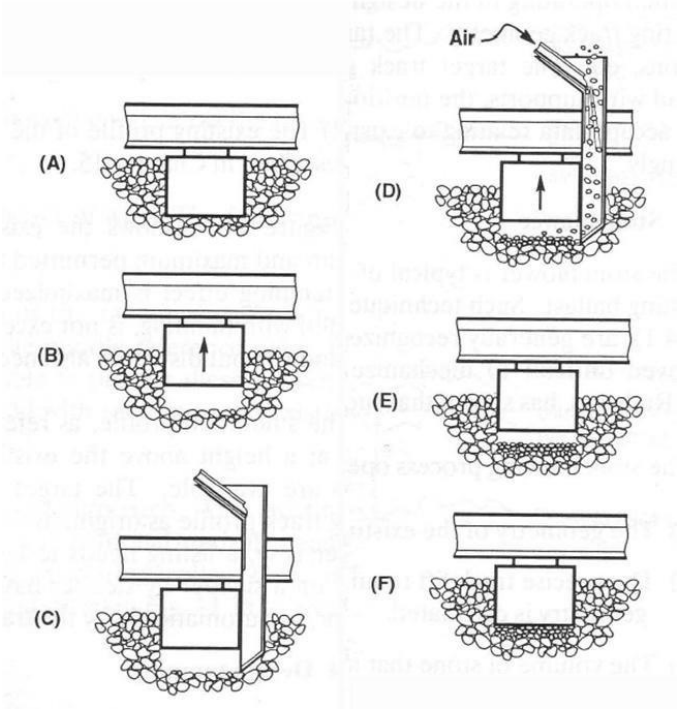

Figure 17. Stone blowing process. (Selig & Waters, 1994).

Undercutting and cleaning of ballast

A machine known as an undercutter/cleaner shakes the fouled ballast through one or more sieves while it separates the large stones from the fine material. This operation involves excavating chain to remove old fouled ballast from the track. The fouling material is wasted while the larger ballast particles that were retained on the sieve are then transported back to the track. This process can be seen in the following figures.

Figure 18. The undercutting operation (Li, Hyslip, Sussmann, & Chrismer, 2015).

New ballast is typically needed to cover the difference since, sometimes, the amount of ballast returned to the track after sieving is insufficient to provide a full-depth ballast section.

The cleaning of stone ballast improves the drainage by removing the dirt and opening up the voids between the stones however this process is expensive, and, in some cases, it is considered more economical to throw away the old ballast to a certain depth below the ties and add new ballast (Li, Hyslip, Sussmann, & Chrismer, 2015).

Drainage

Subsurface drainage systems collect the infiltration water that seeps into the formation, i.e., the top layer, and drawdown the water table level. The drainages can be classified into five types according to their location and geometry: longitudinal drain, transverse drain, drainage blankets, horizontal drains or vertical drains (ARTC A. , 2006).

In order to know which is the most convenient maintenance solution Li, D. et al. (2015) propose the relation between the test parameters with track problem diagnostic and define the maintenance or remedial actions. This is presented in Table 8, where the causes for the deflection of the rail are analyzed.

Parameter	*Problem*	*Maintenance/rehabilitation*
Low track stiffness	Poor or weak subgrade or fouled muddy ballast	Adequate granular layers, improve drainage, stabilize subgrade
Variable track stiffness	Variable track support (stiffness or modulus)	Match stiffness with railseat pad or ballast mat, strengthen weaker subgrade, improve drainage
Void	Fouled ballast, local settlement, or poor fastener condition	Replace broken fasteners, tamp/ surface, stone blow, undercut

Table 8. Track stiffness parameters and potential maintenance needs (Li, Hyslip, Sussmann, & Chrismer, 2015)

According to the Table 8, the reason for detecting a low track stiffness as a parameter, is due to the presence of a poor or weak subgrade condition or due to fouled muddy ballast. The maintenance for this condition includes the reconstruction of the track substructure layers (ballast and subballast) and/or the stabilization of the subgrade.

Variable track stiffness parameter indicates a condition where variation in track support occurs. This can be the case with bridges, tunnels, concrete to wood tie transitions, or when there are changes in local geology. This variation in track support results in track deterioration and settlement. Methods to improve this track condition include design of rail seat pads, under-tie pads, or ballast mats.

Finally, the presence of voids indicates a soft point in the track structure bringing as a result hanging ties (which is a local settlement condition) and possibly fouled ballast. Methods to reduce the void deflection include inspection and repair of broken fasteners, tamping, stone blowing, and undercutting.

The decisions on ballast and subgrade maintenance are subjective and the maintenance frequency increase as the ballast condition deteriorates until the ballast replacement is required. The ballast replacement is necessary right after the ballast archive its highly consolidated states (see Figure 19, part c) because beyond this consolidated state the ballast deteriorates, and the void in the aggregates will be filled with fine material from its breakage. After that consolidated state the ballast loses its mechanical performance, and at this point, the maintenance with tamping will only lead to a totally loosened matrix of ballast therefore the replacement will be necessary.

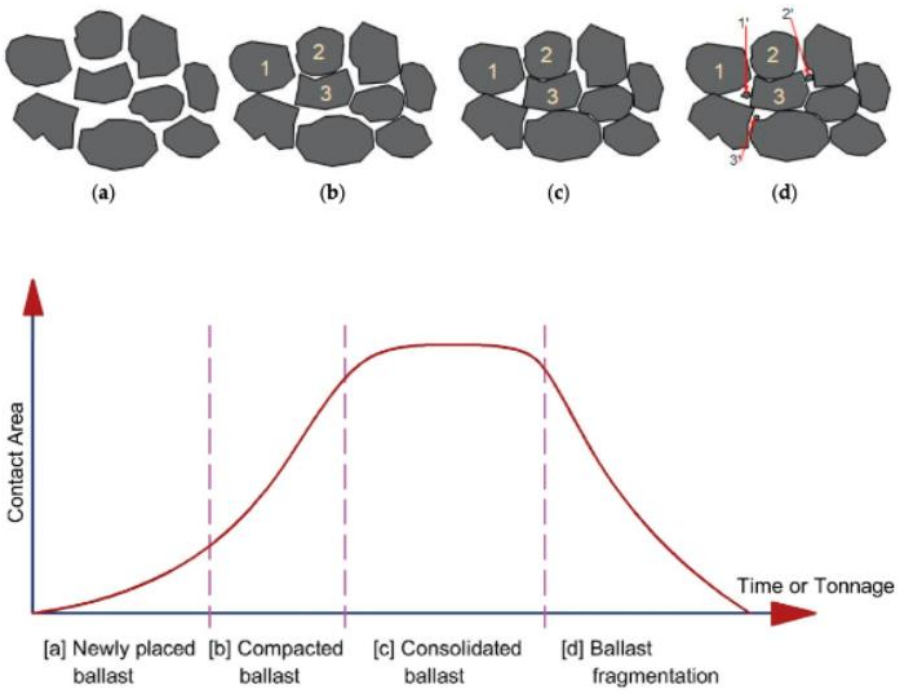

Figure 19. Time and load bound variation in ballast aggregate-aggregate contact area. (Bassey, Ngene, Akinwumi, Akplan, & Bamigboye, 2020).

CHAPTER 2: GROUND PENETRATING RADAR (GPR)

2.1. METHODS TO CHARACTERIZE THE BALLAST

As was just exposed in the previous chapter, the railway ballast is not indestructible and requires regular inspections and maintenance activities. For the inspection of the railway track material, it is commonly used traditional visual inspection. This is a methodology that is still widely diffused nevertheless it will allow to the evaluator to report the state of the railway material only at a superficial level, neglecting the deep pollution and fragmentation of the aggregates at the foundation levels. Consequently, by reeling only on visual inspection the most relevant problems of the ballast as it is the fouling and fragmentation of the material, will be detected only at a very advanced stage (Bianchini Ciampoli, Calvi, & D'Amico, 2019).

Therefore, in order to complement the traditional visual inspection procedure, it is necessary to consider additional techniques. Appropriated tools for field investigation of railway substructure problem include cross trenches, cone penetrometer test, test boring, characterization of track geometry data and deterioration trends, track stiffness measurements, and GPR data measurement (Hyslip, Olhoeft, Smith, & Selig, 2005).

Those field methods to assess the ballast condition can be classified as destructive (cross trenches, cone penetrometer test, test boring) and non-destructive methods (GPR). The first one consists of the excavation of the ballast from the track in order to take samples to be sent and analyses though laboratory test. Recommended location for the ballast sampling from Klassen et al. (1987) are illustrated in the Figure 20. The number 1 and 2 corresponds to the loaded zone beneath the ties while the number 3 and 4 corresponds to the zone between the ties which is not directly loaded. The number 5 correspond to the shoulder of the ballast layer.

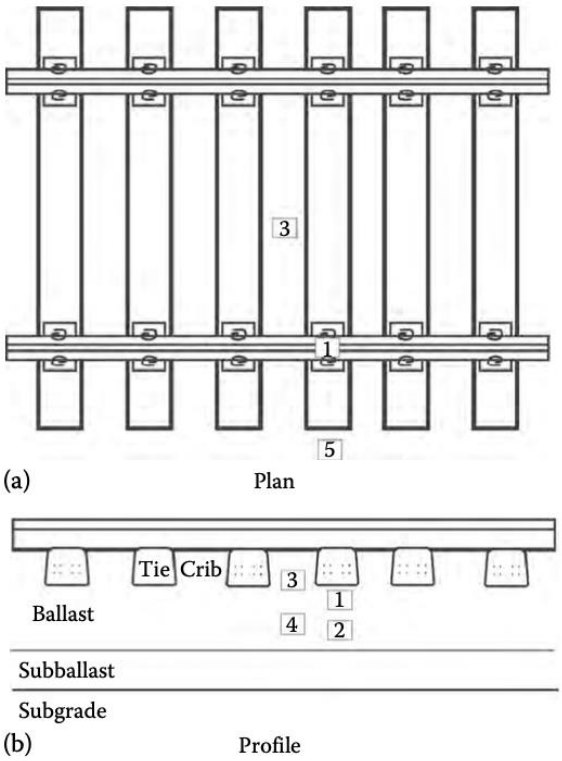

Figure 20. Ballast sample location recommendations. (Klassen, Clifton, & Watters, 1987).

However, this sampling process results to be not only inefficient but also tends to fail to provide adequate information about the substructure of the track since there could exists significant changes in substructure condition along the length of a railway track, even at close intervals, hence quicker and more comprehensive assessment methods are needed (Bassey, Ngene, Akinwumi, Akplan, & Bamigboye, 2020).

Within this context, non-destructive testing techniques are becoming more important in the health monitoring of railways. And among them, the use of microwave systems is becoming popular all around the world (Manacorda & Simi, 2012). Non-destructive test methods include geophysics/ remote sensing, reflection and refraction seismic surveys, magnetic surveys, gravity surveys, resistivity surveys, continuous surface wave tests, electromagnetic (EM) surveys, GPR surveys, infrared, radiometric and light detection and ranging (LiDAR) surveys (Artagan, Bianchini Ciampoli, D'Amico, Calvi, & Tosti, 2019).

The first GPR applications in railway engineering date back to the 1980s and involved low-frequency systems mounted over the rails (Benedetto, Tosti, & Alani, 2017). A large uncertainty respect to those low frequency system was the interpretation of the results; therefore, subsequent applications have focused on the use of high frequency antenna systems (Benedetto A. , Tosti, Bianchini Ciampoli, Calvi, & Brancadoro, 2017). In the past 20 years, many studies have been performed on ballast layer inspection and condition evaluation with GPR (Wang, et al., 2022).

2.2. DESCRIPTION OF GPR TECHNOLOGY

GPR is an efficient and non-invasive tool for mapping railroad structures and analyzing ground conditions (Silvast M. , Nurmikolu, Wiljanen, & Levomäki, 2013). The GPR is a geophysical technique which allows to inspect relevant features of subsurface by using information from the propagation of electromagnetic (EM) fields where the propagation will depend on the characteristics of the device and the properties of the tested materials. (Bianchini Ciampoli, Calvi, & D'Amico, 2019). Thanks to the GPR technology, track bed interfaces can be detected. They are shown as a linear reflection in the GPR data. These reflections will only occur when there is a contrast in the electrical properties of the materials, in particular the dielectric constant.

The GPR systems typically have the following three components (Saarenketo & Scullion, 2000):

1. a pulse generator which generates a single pulse of a given center frequency and power,
2. an antenna which transmits the pulses into the medium and captures the reflected signal, and
3. a sampler recorder which collects the reflected signals and converts them into a form for computer storage.

The principle of GPR is shown in this Figure 21, where it is illustrated the emission of EM waves inside of ballast layer by the transmitting antenna.

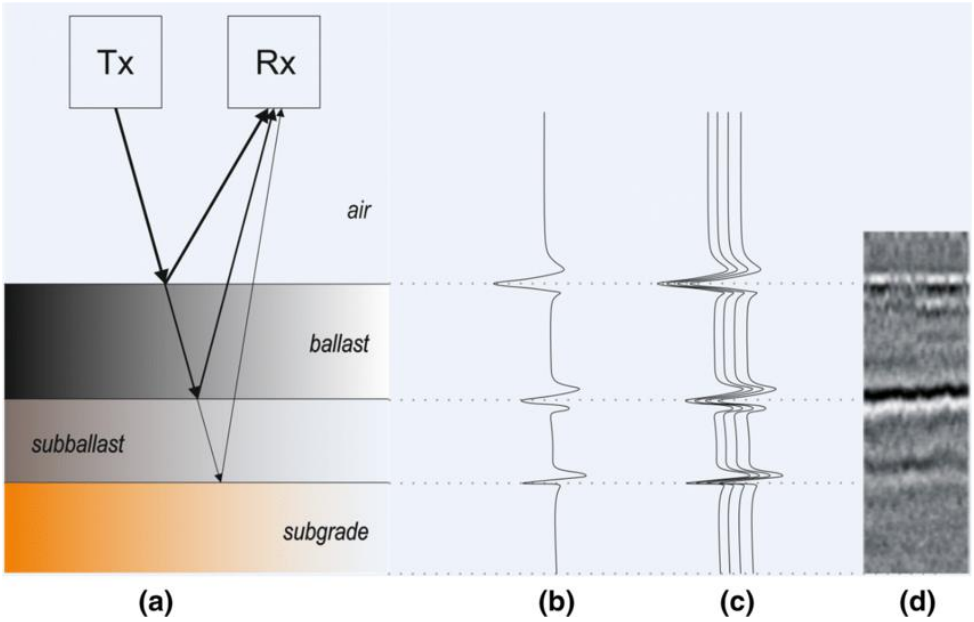

Figure 21. The generation of a GPR profile with an air-coupled antenna on a track-bed. (a) The transmitted energy is reflected from the boundaries in the substructure. (b) a single trace with reflection amplitudes for the reflection interfaces in a. (c) a sequence of multiple scans. (d) adjacent scans combined to build a B-scan (Hyslip, Olhoeft, Smith, & Selig, 2005).

The EM wave travel though the soil and the energy is partially absorbed and partially reflected (Figure 21, a). The reflection occurs when the waves encounter a boundary layer or area with different dielectric properties. The trackbed interfaces are show as a linear reflection in the GPR data. These reflections will only occur where there is a contrast in the electrical properties of the materials, for example between a clean ballast layer and subgrade or clean ballast and a fouled ballast layer.

After that, the receiver antenna records the return wave time and amplitude to form a single waveform (Figure 21, b) which are obtained along the railway line. The collected information is then down-converted to a low-frequency signal such that they can be digitized by a conventional analog-to-digital converter for further processing and display. The wave form information can be gathered to form a 2D radar image called radargram (Figure 21, d).

Lastly, by analyzing both the single waveform signal and the 2D radar image in terms of time delay, the amplitude of the reflection peaks and the modulation of frequency, main features of the material can be predicted (Artagan, Bianchini Ciampoli, D'Amico, Calvi, & Tosti, 2019). It can be obtained indicators that can reflect ballast layer thickness, ballast fouling level, and drainage (Wang, et al., 2022).

The data obtained from a GPR survey can be summarized in terms of information that can be obtained on the thickness and depth of layer, so called layer metrics, and information on the quality of the ballast layer, in the form of a ballast fouling index (Eriksen, Gascoyne, & Fraser, 2011). Layer metrics includes the ballast depth and the Layer Roughness Index (LRI) which indicates the degree of variance in the thickness in a layer. This last one is use to identify sub-grade failure or wet bed formation which can be the interpretation of rapid variations in the LRI.

Antenna choice for the GPR survey

One of the main components of the GPR system are the antennas. The Antennas are designed to operate at various frequencies from tens of MHz to several GHz. The antenna choice must consider that higher frequency antennas provide results at a better resolution, however the depth of penetration is more reduced compared to those low frequencies antennas. For low frequency antennas choices, even though they can reach deeper investigation distance, the resolution of the result is reduced.

The second consideration for the antennas is the type. The most common radar antennae use in the GPR test fall into two broad categories: air-launched horn antennae and ground-coupled dipole antennae (Benedetto A. , Tosti, Bianchini Ciampoli, Calvi, & Brancadoro, 2017). Air coupled antennas are design to be used suspended above the ground surface while ground couple antennas are designed to be in direct contact with the ground surface. The last one allows a deeper penetration in the medium.

However, for railway application, the antenna must be used lifted up in order to be not damaged by obstacles during measurements (e.g., switches, crossings, gravel between sleepers), additionally strong echoes produced by the rails may hide weak signals coming from railway bed (Manacorda, Morandi, Sarri, & Staccone, 2002). Causing misreading of the signal and inaccurate measurements of the state of the ballast layer.

The South African Railroad, Spoornet (Vorster, 2012), compared the use of air and ground coupled antennas to determine and evaluate the level of ballast fouling in the track. They conclude that the air coupled antennas have significant advantages respect to the ground antenna including less noisy data and the ability to deploy the antennas high enough to clear any obstacles associated with the track. While for the

ground couple antenna there is a potential problem of interference of the rail and ties with energy transmission. They can produce ringing when used not in contact with the surface of the material to be inspected. This last type of antenna worked best when they are in direct contact with the ground surface and, for railway inspection where it is required large travelling distances along track, it was not found to be feasible since the vibrating of the antenna was potentially detrimental to the data and equipment. Therefore, that the ground coupled antennas may need further development to improve operation when deployed above the ground (Theodore & Sussmann, 1999).

In particular, for railway applications, air coupled antennas are typically employ (Li, Hyslip, Sussmann, & Chrismer, 2015). In the Figure 22 is presented a GPR setup with 3 pairs of horn antennas. The description and the characteristics of these type of antenna is given by Benedetto et al. (2017). The air coupled antennas normally work mounted on a mobile vehicle and are suspended at a certain distance from the surface about 15 to 50 cm. They perform measurements at traffic speeds (up to 80-120 km/h) without any interference with traffic. The frequencies range from 1 to 2.5 GHz, corresponding to penetration depths in the order of 1 m to 0.4 m, respectively. With central frequencies of typical 1 GHz. The data collection speed can be up to 100 scans per second which means that the distance between one scan and the next one is 33 cm approximately.

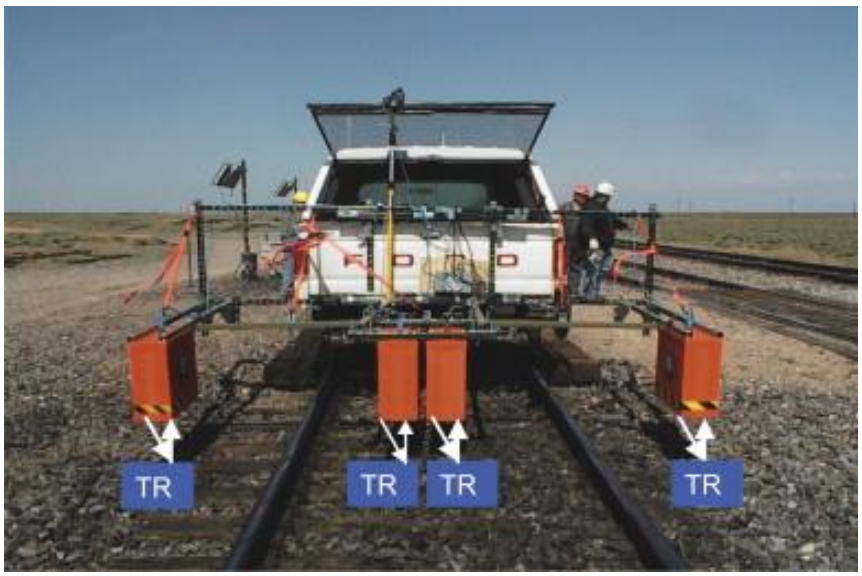

Figure 22. GPR Hi-Rail Setup with 1 GHz Horn Antennas (TR = Transmitter and Receiver). (Al-Qadi, Xie, & Roberts, 2008)

The propagation of the electromagnetic waves

The propagation of EM waves in the ground medium follows Maxwell's equations (Eq. 10, Eq. 11). Thanks to those equations, it can be providing a description of the production and interrelation of electric and magnetic fields.

$$\nabla E = -\mu \frac{\partial H}{\partial t} \qquad \textit{Eq. 10}$$

$$\nabla H = \varepsilon \frac{\partial E}{\partial t} + \sigma E \qquad \textit{Eq. 11}$$

Where E is the electric field strength, H is the magnetic field strength, ε is the dielectric constant, μ is the magnetic permeability and σ is the electrical conductivity. The EM behavior of a material is governed by its dielectric properties, i.e., the dielectric constant (influencing the wave velocity), the electric conductivity (affecting the wave attenuation), and the magnetic permeability (Benedetto, Tosti, & Alani, 2017).

In this order of ideas, the travel time of the GPR signal can be collected in the field, however, the velocity of the wave in the medium is variable and will depend on the dielectric constant of the material. The dielectric constant characterizes the ability of a medium to be polarized by an electromagnetic field (Wang, et al., 2022). Once the dielectric constant is known, the relative EM wave propagation velocity can be computed (Eq. 12). More specifically, the dielectric constant and the propagation speed of electromagnetic waves in a vacuum (c) are used to determine the speed of electromagnetic wave propagation (υ) in the medium, as shown in the next equation (Daniels, 2004).

$$\upsilon = \frac{c}{\sqrt{\varepsilon}} \qquad \textit{Eq. 12}$$

Once the EM wave propagation velocity is known, the depth of the object or interface can be computed as follows (Eq. 13).

$$d = \upsilon \cdot \frac{t}{2} \qquad \textit{Eq. 13}$$

Where d is the depth of the object or layer of interest and t is the two-way travel time of the signal to and from the target (Daniels, 2004).

An important parameter to define in the GPR system is the time window. The time window is defined as the time the receiver antenna listens and records the echoes from a transmitted electromagnetic pulse. In other words, the time window defines the total trace length of the investigation. It is important to note that choosing a time window that is too short may cause the loss of important information of the ground since the system might stop listening and recording before the signal has reached the desired target depth. In the other side, choosing a time window that is extremely long will cause large size of the files that may be unnecessary. The time window is often expressed in nano seconds (ns) and together with the velocity (m/ns) of the electromagnetic pulse in the investigated media it can provide the operator with a total investigation depth (in meter) (Read, Meddah, Li, TTCI, & Mui, 2017).

The relation between the time window, layer thickness and ballast dielectric constants can be appreciated in the Figure 23 where is presented the calculated layer thickness against ballast dielectric constants (ε) for wave travel times of 5, 15 and 30 ns. Notice that for longer time travel, more sensitive the thickness calculation is to the ε value. Notice also in the curve of 30 ns (green line) that the value of thickness varies 20 m approximately when the dielectric constants vary from $\varepsilon = 3\ to\ \varepsilon = 5$.

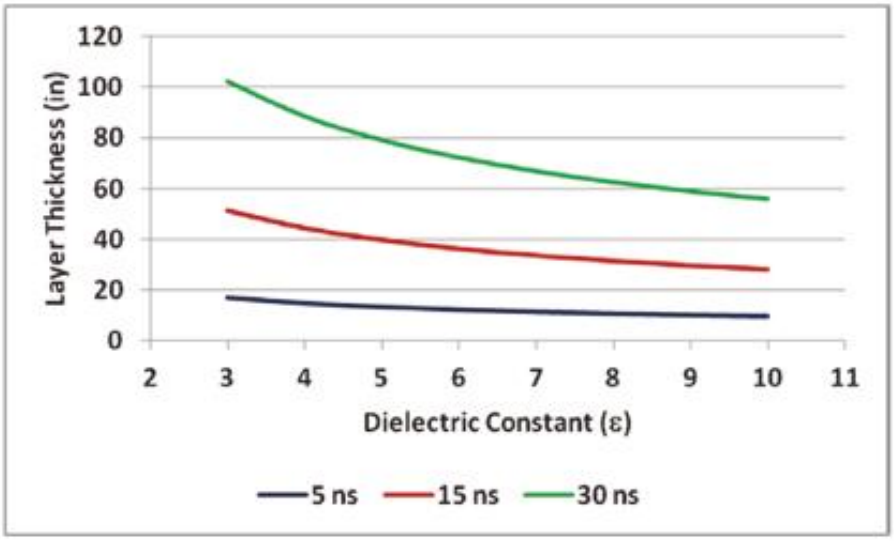

Figure 23. Sensitivity of the thickness calculation to travel time and material dielectric constants (Read, Meddah, Li, TTCI, & Mui, 2017)

2.3. GPR APPLY FOR THE BALLAST CHARACTERIZATION

In particular for the ballast layer, according to Silvast et al. (2013) the GPR has shown its ability to determine layer thickness values, analyze the quality of materials in the structural layers, such as the fouling of ballast, to determine track substructure conditions such as layer deformation, drainage problem and determination of the material quality parameters. This is done by recording variations of a reflection amplitude, changes in the arrival time of specific reflections, and changes in the signal strength. In this section is going to be treated in more detail, by citing study cases, how the GPR can assess the ballast state.

Dielectric constant of the ballast

As was mentioned before, the dielectric constant is a critical factor which defines most of the behavior of the reflection of the materials encountered in the ground. This value will vary depending on the material of the ballast aggregate and the fouling contaminant.

Clark, M.R., et al. (2001) carried on laboratory experiments in a brick tank considering two types of ballast: clean and spent. The ballast was compacted in layers as it was placed into the tank to simulate as much as possible in site conditions. The clean ballast was granite crushed, uniformly graded, free from all kinds of dirt with a high abrasiveness resistance value and high aggregate toughness value. The spent ballast used came from a track bed that was considered to be at the end of its usable life. The Figure 24 and Figure 25 shows the result of the sieve analysis of the clean and spend ballast respectively.

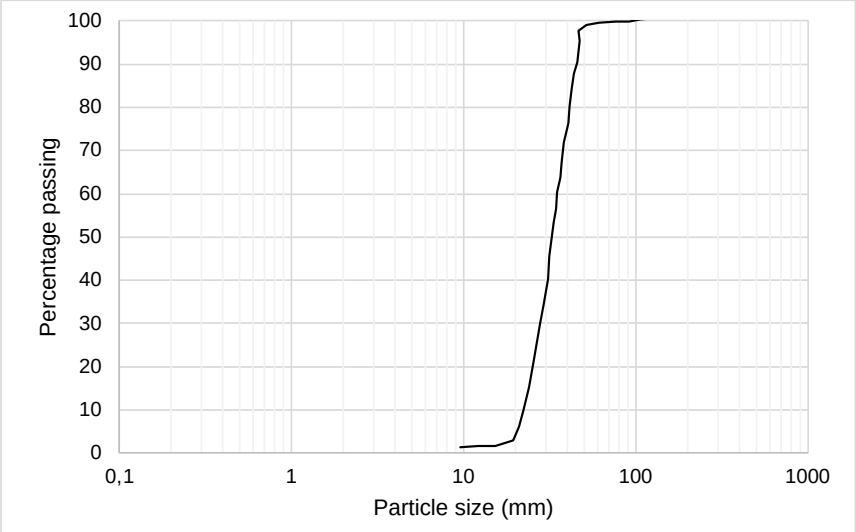

Figure 24. Sieve analysis of clean ballast (Clark, Gillespie, Kemp, & McCann, 2001).

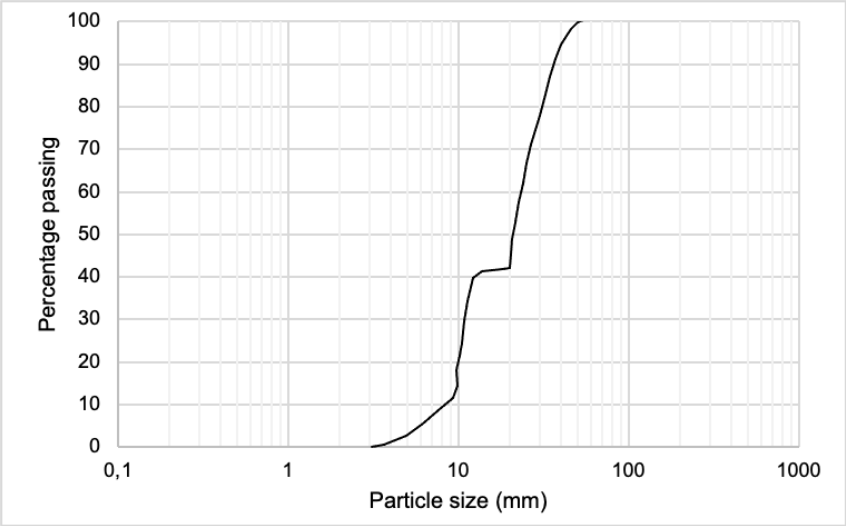

Figure 25. Sieve analysis of spent ballast (Clark, Gillespie, Kemp, & McCann, 2001).

In the study 500 and 900 MHz ground coupled antennas were used. The results from the test of the value of the dielectric constant of the ballast at different conditions are summarized in Table 9.

Material	ε_r	Velocity (m/s)
Air	1	3.00×10^8
Water	81	0.33×10^8
Dry clean ballast	3.0	1.73×10^8
Wet clean ballast (5% water[a])	3.5	1.60×10^8
Saturated clean ballast	26.9	0.48×10^8
Dry spent ballast	4.3	1.45×10^8
Wet spent ballast (5% water[a])	7.8	1.07×10^8
Saturated spent ballast	38.5	0.58×10^8

[a] 5% water by volume added.

Table 9. Dielectric constant and velocity for ballast (Clark, Gillespie, Kemp, & McCann, 2001).

From the experiments it was concluded that the dielectric constant of the dry clean ballast was 3 while the dry spend ballast was 4.3. The reason behind that is because the spend ballast has a finer well-graded particle size, which means less air voids, giving as a result a higher dielectric value and lower velocity of propagation compared with the clean ballast (Clark, Gillespie, Kemp, & McCann, 2001).

During the test it was also analyzed the change in the dielectric constant by increasing by 5% the water content in the sample. It was found that the dielectric constant is higher when water is added to the material. The reason behind that is that the speed of the EM shear waves through water are very slow ($0.33\ x\ 10^8\ m/s$) compared to that of the air. Therefore, in the wet ballast the characteristics of the water will be predominate in the EM response, due to the fact that the water will be replacing the air in the voids. This was confirmed by the experiment when 5% water was added to the spent ballast. Here was observed a 45% increase in the dielectric value of the material. It is important to mention that the increase of the dielectric value was higher for the spend ballast with 5% of water than that of the clean ballast with the same percentage of water added. The reason for that is because the spent ballast has a higher capacity for water retention due to the high fines content.

Another study was made by Leng, Z., & Al-Qadi, I.L. (2010) analyze the dielectric constant of the ballast considering two common ballast types of material: granite and limestone. The samples were studied under various fouling and moisture conditions. It is important to mention that the fouling material was clay. Both samples were uniformly graded with an aggregate size of 63.5 mm with air voids after compaction

of 36.3% for granite and 37.8%. They determine though control laboratory test the dielectric constant using 2 GHz air coupled antenna. The results of the study are presented for the variation in the dielectric constant at different fouling level and for different moisture content in the Figure 26 and Figure 27 respectively.

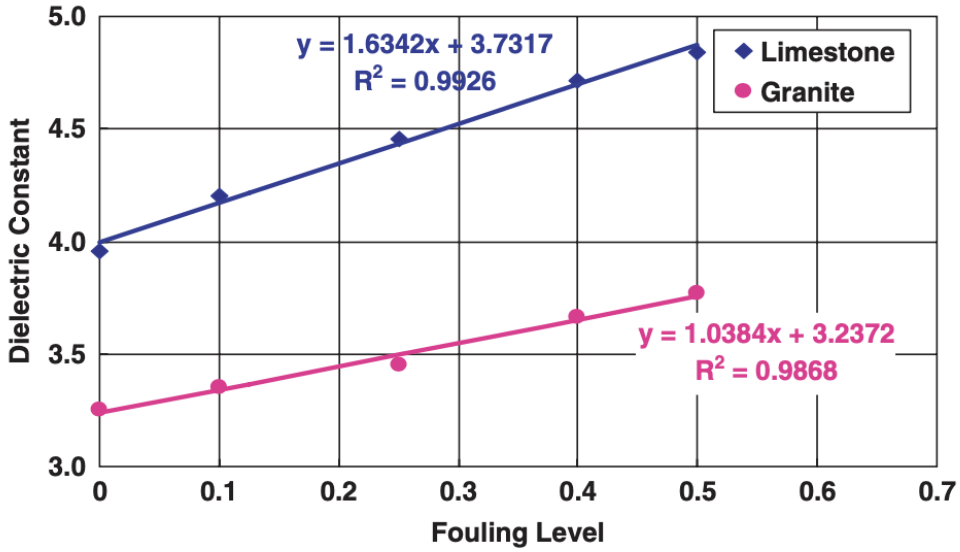

Figure 26, Dielectric constants of ballasts fouled by various percentages of dry clay (Leng & Al-Qadi, 2010).

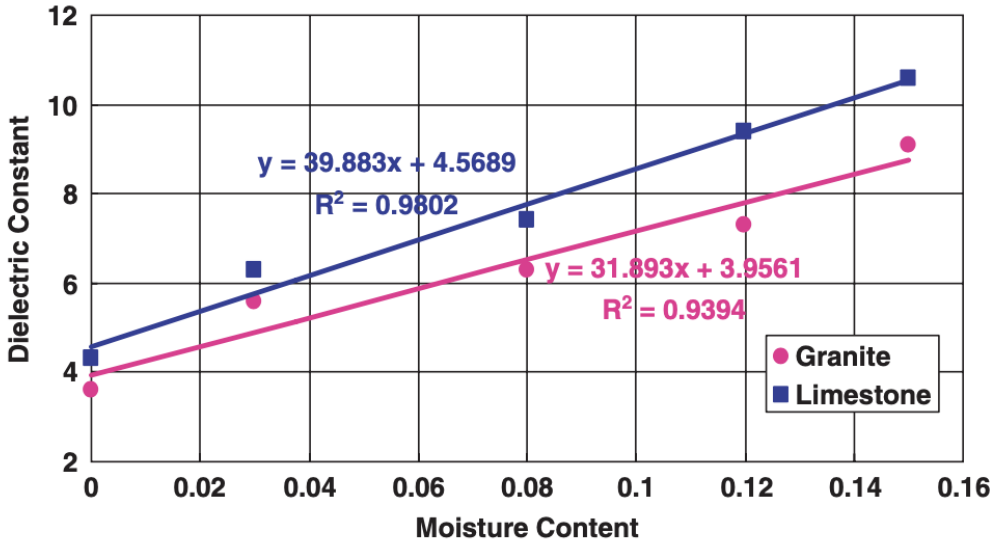

Figure 27. Dielectric constants of ballasts with 13% fouling at by various moisture contents (Leng & Al-Qadi, 2010).

The Figure 26 presents the results of dielectric constant under dry condition at various fouling levels for both materials: granite and limestone. It could be concluded through the results that the granite ballast has a smaller dielectric constant than limestone for the same fouling level. The dielectric constant for the clean ballast is 3.25 for granite and 3.96 for limestone. Also, the dielectric constant increases with the increase in the fouling level, here is presented a variation of the dielectric constant that ranges from 3.25 to 3.77 and 3.96 to 4.84 for granite and limestone ballast respectively, between 0 and 50% con fouling level. In fact, there is a linear relationship in the ballast dielectric constant and the fouling level for both ballast materials. For any fouling level between 0 and 50%, the equations shown in Figure 26 can be used to predict the dielectric constant of dry ballast. Only if the fouling material is clay and for the type of ballast material specified.

The Figure 27 displays the measured dielectric constants of ballast with 13% fouling material at various moisture contents. From that it was concluded that as the moisture content increases, the dielectric constant of the ballast increases significantly. When the moisture content by volume of air void increases from 0% to 15%, the increases in the dielectric constants are from 3.9 to 9.1 and from 4.2 to 10.5 for granite and limestone respectively. Again, there is a strong linear relationship between the dielectric constant and the moisture content express in the equation presented in the Figure 27.

As it can be noticed from those two previous study cases, the water is the determining factor for the dielectric constant of the ballast layer. The clean ballast has a greater volume of air voids which lowers the average dielectric constant of the medium while the water increases the average dielectric constant of the medium (De Bold, O'Connor, Morrissey, & Forde, 2015). Thanks to that behavior of the materials with the water, the drainage capacity of the ballast can also be studied with the GPR and is going to be analyze in the next paragraphs.

Detection of water trap in the ballast layer

The ability of the GPR to detect moisture area were studied by Manacorda, G. et al., (2002). They use multi-frequency antenna of 200 and 600 MHz, with range depth of 60ns and number of samples per scan up to 512. The antenna height was 25 cm from the ground and the data collection speed was 80 km/h. From the results, it could be concluded that the GPR accurately located the damaged track sections. In particular, the GPR can detect moist area in the ballast layer, and it is presented in

the signal as a strong reflection as it can be seen in the Figure 28 at the left. Additionally, in the middle of the image, there are some echoes produced by stones placed just above the subsoil. The reason for the stones is to provide strength for the subsoil and this is a common solution when soft soil is present.

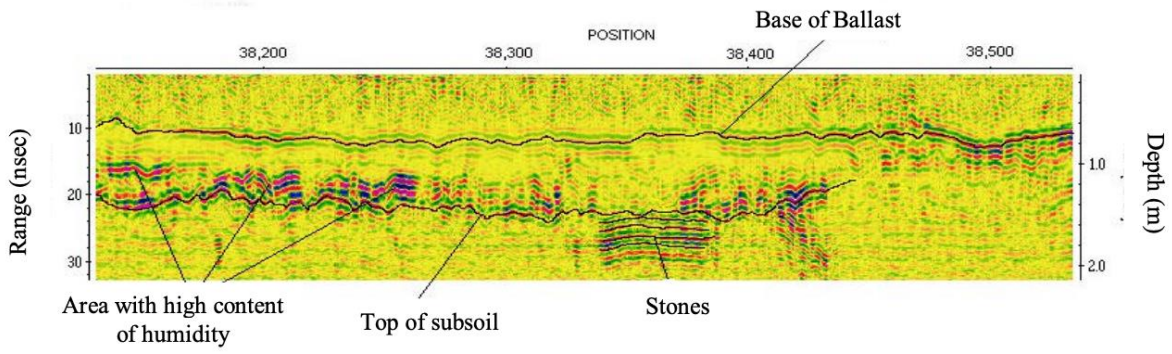

Figure 28. Moist area detection with GPR (Manacorda, Morandi, Sarri, & Staccone, 2002).

Another study by Li, D. et al. (2015) shows the capacity of the GPR detecting moisture in a track resulting from a wetting test in Massachusetts. In the Figure 29 it is evident how the moisture is changing as the fouling remains the same. Initially, in the part “a” there is no water added however a little moisture is detected in the gage of track. In the following condition “b”, water is poured in the track, and it is evident an increase in moisture identify by a stronger reflection in the signal. Finally, in the part “c” the intensity of the reflection is reduce and this can be interpreted as the drainage of the water from the track.

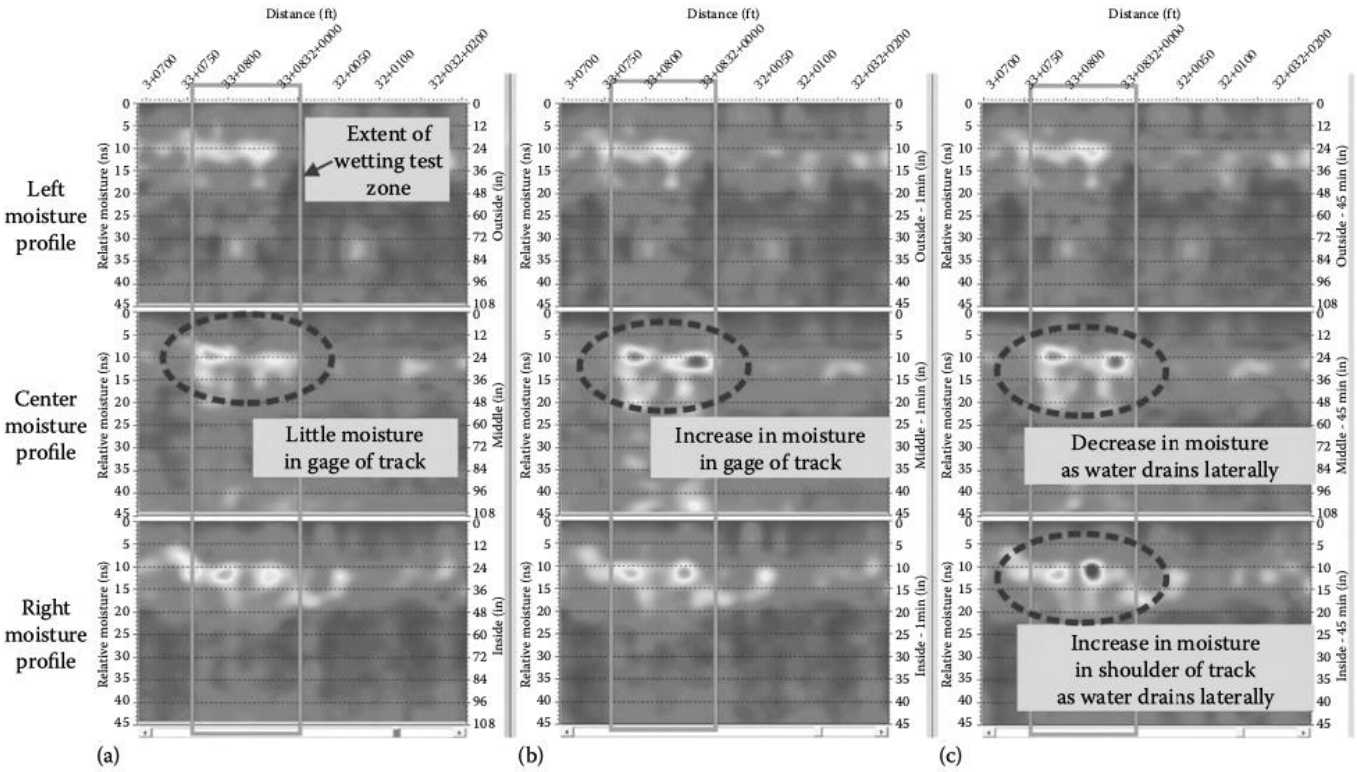

Figure 29. Results from wetting test showing change in moisture: (a) no water added; (b) 2 minutes after water added to center of track; and (c) 45 minutes after water added to center of track. (Li, Hyslip, Sussmann, & Chrismer, 2015).

In a similar manner to ballast fouling, moisture affects the GPR signal content at distinct frequencies (Li, Hyslip, Sussmann, & Chrismer, 2015). Therefore, despite of the sensitivity of the GPR to the moisture content, this cannot be discriminated from the fouling content since they affect the signal in a similar way. The presence of water evidently has a stronger influence on the surface reflectivity, but it is not possible to distinguish between ballast that is highly contaminated (with dry fines) from ballast that has low fines contamination but retains a moderate amount of water based on the surface reflection amplitude (Barrett, Day, Gascoyne, & Eriksen, 2019). Additionally, in many cases, zone of fouled ballast coincides with pockets of trapped water (Theodore & Sussmann, 1999).

Nevertheless, with the GPR data it can be located track substructure changes, and this allows the targeting of the test boring in a more efficient way to determine the causes of the substructure degradation.

Scattering analysis for the fouling assessment in the ballast layer

In track maintenance management programs, GPR has been used to evaluate the state of the railway track's substructure (ballast, subballast, and subgrade) and to provide quantitative indices of substructure condition (Hyslip, Olhoeft, Smith, & Selig, 2005). In fact, it has been proved that the laboratory fouling results and GPR fouling index correlate well, and thanks to the GPR fouling index score, it is possible to describe the condition of the railway substructure at each kilometer, which helps to effectively select the sections for ballast cleaning process. (Silvast M. , Nurmikolu, Wiljanen, & Levomaki, 2010).

The fouling can be evaluated by the signal scattering. The scattering occurs when the dimensions of particles or inclusions in a material are on the same order of scale as the EM wavelength. This is the case when the signal pulse travels through clean ballast aggregate, here a resonance behavior is observed in the GPR high frequency response. The source of the scattering is called scatter and for the railway ballast, the scatters are the air voids between the ballast particles (Zhang, Eriksen, & Gascoyne, 2010). This theory stands as long as there is air in the ballast void spaces. When these spaces become filled up with fine particles, the scattering response disappears. When the ballast material presents any type of void contamination, this will result in the absorption of GPR energy, therefore, a reduction in the amplitude of the scattered energy will be observe in the data results (Wang, et al., 2022).

Typically, the size of the voids in clean ballast varies from 11mm to 29mm which results in a dominant scattering response at frequencies of around 2GHz (Selig & Waters, 1994). Same conclusion, respect to the antenna frequency to better detect the scattering of the signal, was obtained in a field GPR survey with multiple sets of 1 and 2 GHz air-horn antenna made by the Transportation Technology Center, Inc. (TTCI) in Pueblo, Colorado. It was found that 2 GHz is more sensitive to the change in scattering pattern while the void scattering is barely observable in 1GHz data (Al-Qadi, Xie, & Roberts, 2008). This conclusion is illustrated in the Figure 30 where is compare the data obtained with the two antennae.

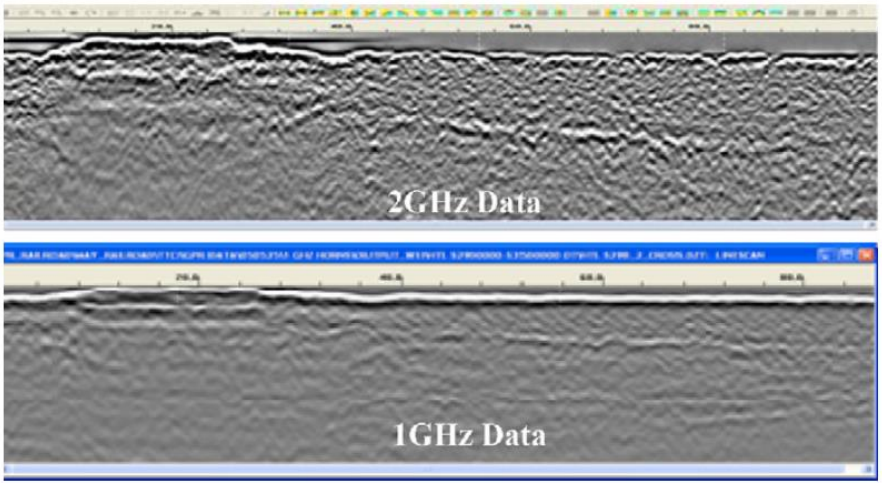

Figure 30. Longitudinal GPR images obtained with 1 and 2 GHz antennae (Al-Qadi, Xie, & Roberts, 2008).

The selection of the antenna for the scattering analysis was also studied by Barret, D. et al., (2019). The Figure 31 presents the scattering efficiency for different sizes of voids in the ballast layer. It is illustrated that the scattering efficiency is reduced as the size of the air voids decreases. This also will depend on the bandwidth. At 400 MHz, void size would need to be 50 mm in radius (black continuous line in the Figure 31) or larger to produce a strong scattering signal, while by using 2 GHz antenna, the scattering signal would reduce in strength as the scatterer size reduces below 10 mm radius.

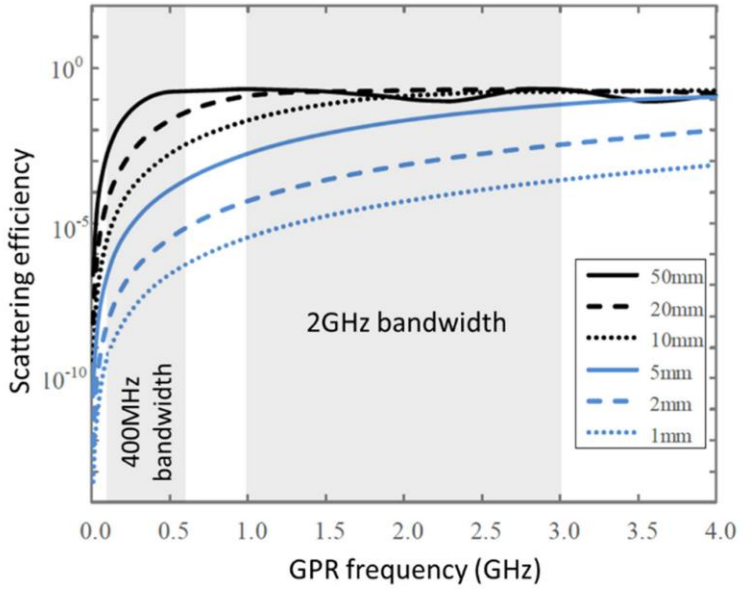

Figure 31. Scattering efficiency for different sizes of voids in ballast layer (Barrett, Day, Gascoyne, & Eriksen, 2019)

In the 2 GHz frequency range, the scattering efficiency is approximately 100,000 times higher for void sizes in the range of 5–20 mm than for void sizes in the range of 1–2 mm (Wang, et al., 2022). Therefore, by using 2GHz bandwidth, the voids filled by fouling are accurately detectable thanks to the fact that the electromagnetic wave scattering response decreases. Finally, this behavior provides the possibility of evaluating the fouling level through analysis of the scattered signal within the ballast layer.

A study case that applies the scattering signal analysis to determine the fouling and the thickness of the clean ballast layer was carried out in United Kingdom, where Barret, D. et al., (2019) determined the time range of the scattered signal recorded with a 2 GHz ultra-wide band horn antenna. Then the measured time range was converted to a depth using an average signal propagation velocity. The results are presented in the radargram in Figure 33. The radargram shows a section of track bed with varying ballast condition. The vertical axis represents depth from the ballast surface modelled using the calibrated signal velocity through clean ballast 152 mm/ns, Additionally, in order to validates the results from the GPR, they took samples by driving steel tubes into the ballast to a depth of 400 mm as is illustrated in Figure 32. After that, the ballast was manually extracted and the depth of the ballast in the absence of any fouled ballast was recorded. This is represented as a black line in the radargram in Figure 33.

The explanation of the different sections in the radargram is describe next.

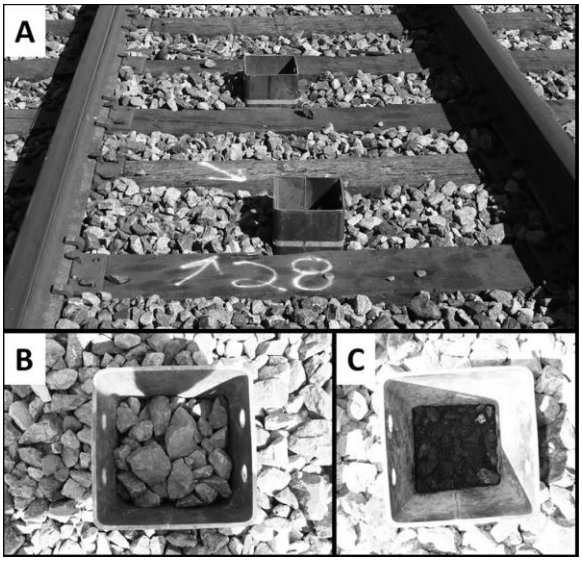

Figure 32. Sampling for clean ballast thickness validation using steel tubes driven into the ballast (Barrett, Day, Gascoyne, & Eriksen, 2019).

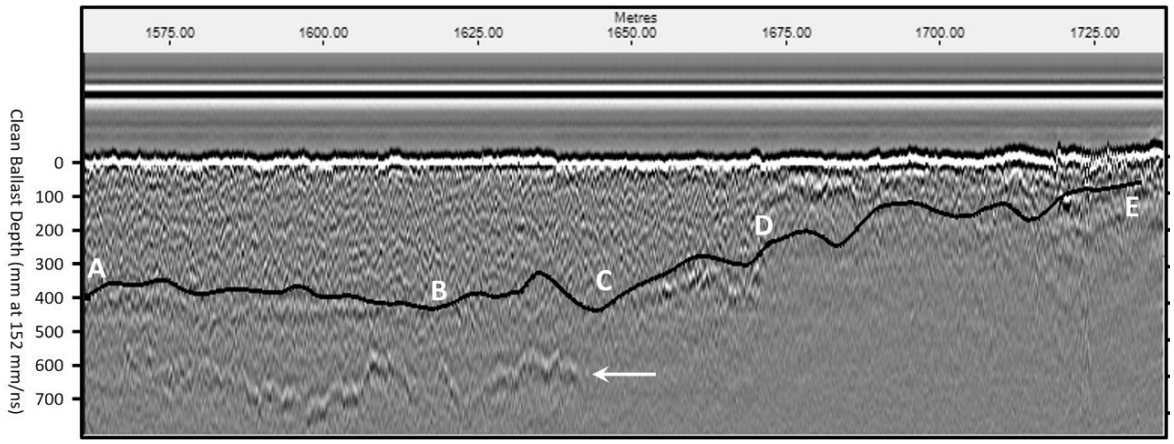

Figure 33. Example of the modelled clean ballast thickness (black line). A bright base-of-ballast reflection is indicated by a white arrow. Letters identify distinct zones of different track bed condition (Barrett, Day, Gascoyne, & Eriksen, 2019).

Section A-B represents high quality ballast with the clean ballast thickness identified as 400 mm (170 mm clean ballast below base of sleeper). The interface at the base of the clean ballast is relatively flat and a reflection can be perceived. Additionally, there is a deeper reflection point by the white arrow, this indicates low levels of signal attenuation and is likely represents the base of ballast.

After that, the section B-C is also representing a high quality ballast, having a similar thickness of clean ballast as section A-B. The difference of section B-C from A-B is that the section B-C has no recognizable reflection at the base of the clean ballast. However, thanks to the scattering analysis, it is possible to identify the thickness of the clean ballast.

The section C-D shows a clean ballast layer that thins from 450 mm to 250 mm over a distance of 25m. The boundary can be easily identified by a bright reflection.

Finally, section D-E represents a poor quality ballast, having a clean ballast thickness of 150 mm (i.e., fouling to a level above the base of the sleepers). The identified interface does not coincide with any reflection event, therefore, just as was mentioned for the section B-C, the scattering analyses helps to identify this boundary of clean ballast material.

As a conclusion to this study, Barret, D. et al., (2019) found a very good correlation between the GPR information and the real sample. According to the study just exposed, we can conclude that the ballast fouling levels, and thickness of fouling layers can be detected by the GPR technology.

Another study carried on by Roberts, R., et al., (2007) used GPR horn antennas to evaluate the railroad ballast conditions in the United States. The data along the track were collected using three 2 GHz antennas; one in the center and the other two at 15 cm from the end of the sleepers. After that, the data was processed and the fouling condition were assessed. Additionally, ground truth data have been compared to the processed GPR data. It is worth to mention that the GPR data presented in the next figure were obtained in a dry environment with stable, sandy subgrade.

In the Figure 34 present the minimally processed data, fully processed data with color coded, and the cross trenches that were dug for ground truth with its respective fouling index (FI) and percentage of moisture (PM) that were determined in laboratory, for four locations in the track. A separate analysis was performed using dynamic cone penetrometer (DCP) data where the fouling of the ballast was identified. The results are represented in the next figure as a horizontal color line in the ground truth data.

It can be notice that the scattering response from the clean ballast is clearly evident in the minimally processed data and there is a good agreement between the depth of clean ballast calculated from the GPR data and the cross-trench ground truth observed. Also, in the minimally processed data, no evident boundary can be observed between fouled ballast and clean ballast. However, the presence of a reflecting boundary is not necessary to determine ballast fouling.

As a conclusion of this study case the authors stated that the comparison shows good agreement between GPR data and ballast condition assessed via ground truth. Furthermore, it was concluded that the 2 GHz horn antennas provide data that are very sensitive to the scattering from void space in clean ballast (Roberts, Al-Qadi, Tutumluer, & Kathage, 2007). The restriction of those antennas is the depth of penetration (60 cm approximate), therefore, for further investigation in the subballast and subgrade layers, lower frequency antennas have to be implemented.

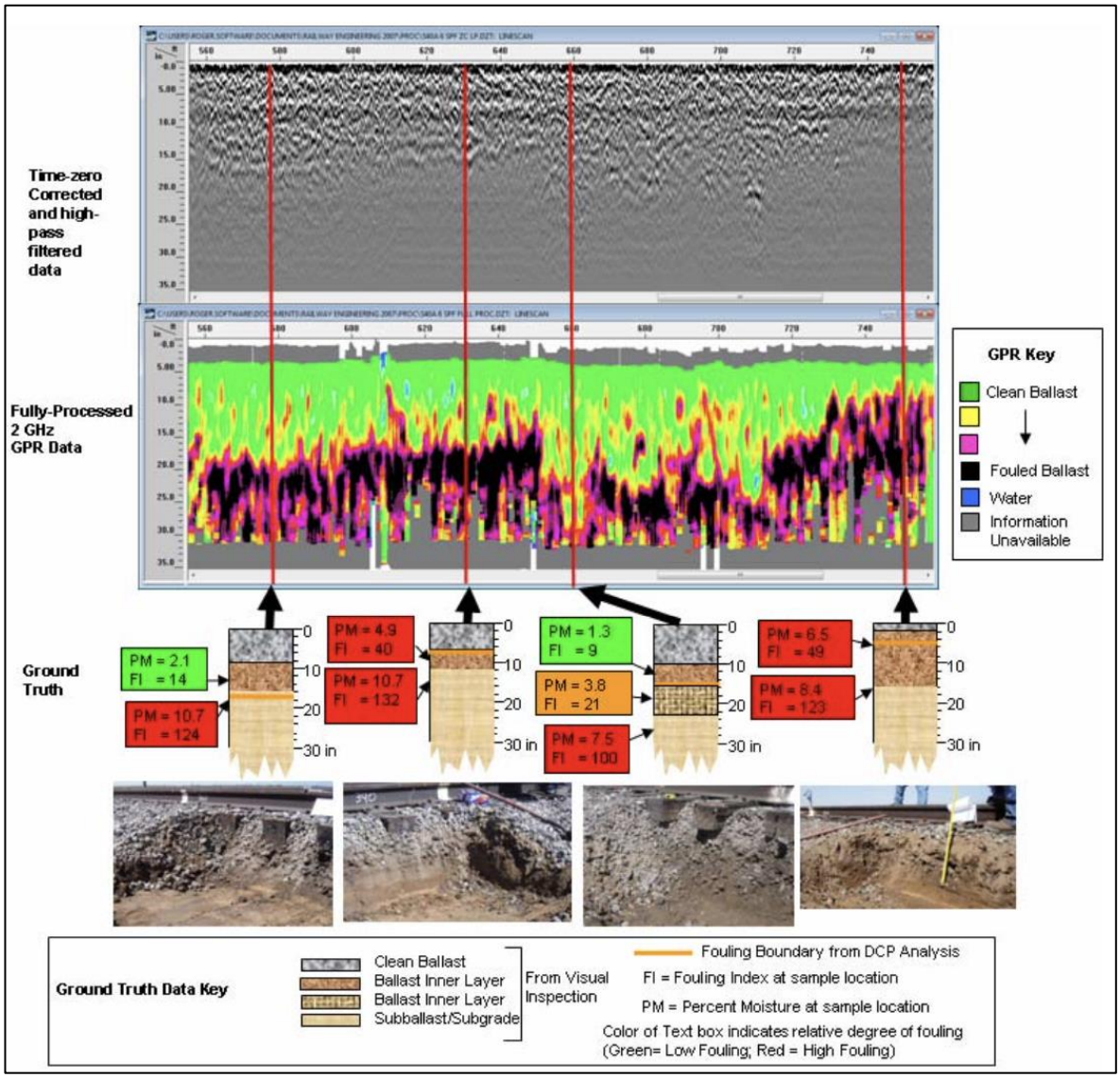

Figure 34. Comparison of minimally processed data (top), fully-processed data (middle), and ground truth (bottom) from a section of track at TTCI. GPR depth values obtained using 6 in/ns (15 cm/ns) propagation velocity. (Roberts, Al-Qadi, Tutumluer, & Kathage, 2007)

To conclude this section, it is worth to mention that, according to Hyslip et al. (2005), the majority of the track substructure problems in the United States can be summarize in the Table 10. The GPR has the ability to detect most of those structural problems. The same table summarizes the substructure problem and the corresponding GPR information that can be measured for defining the extent and severity of the problem.

Substructure Problem	GPR Information Based On
Poor drainage – trapped water	Intensity of GPR reflection and moisture contents of ballast/subballast layers
Poor drainage – layer depression (bathtub)	Difference in depth to impermeable subgrade surface laterally across the track (i.e., lateral layer thickness variation
Fouled ballast	GPR scattering pattern textures and permittivity of ballast layer
Subgrade failure or deformation	Ratio of layer thickness and/or subgrade surface depth from middle to edge of tie. Also, moisture content and consistency of subgrade soil along with thickness of granular layer.
Subgrade attrition	Lack of subballast layer in combination with fine-grained fouling
Subgrade excessive swelling and shrinking	Variation of clay subgrade surface. Also, moisture content and consistency of subgrade soil.
Longitudinal variation of the condition	Variation (roughness of layer thickness, moisture content and composition.
Subballast moving laterally on thin clay surface	Change in layer thickness laterally across the track and presence of high moisture content layer
Transitions	Rate of variation of the substructure layers along or across track of layer properties

Table 10. Substructure problems and corresponding GPR Measurement (Hyslip, Olhoeft, Smith, & Selig, 2005)

2.4. INCORPORATING GPR INSPECTION AND TRACK GEOMETRY

In order to achieve the desired information, so as to be able to correctly characterize the ballast in the railway system, the collected data must be processed. This process can be done by using GPS system, removing unwanted background and applying time-space filters.

It is convenient that the information obtained by the GPR technology is integrated with other information such as track geometry, track stiffness measurements and maintenance records in order to accurate asses the state of the ballast layer and to stablish adequate managing and maintenance program. Combining track geometry measurements with GPR provides unique condition-based information to plan a holistic ballast and track bed management strategy (Eriksen, Gascoyne, & Fraser, 2011). This combination of information can also be used to identify correlations or develop combined index.

One example of a combine index is the QI2 track quality index that was develop for the Irish Rail in 2008 presented by Eriksen, A., et al. (2011). This index is based on the condition for both ballast layer and track geometry which indicators are called combined track quality index (CTQI) and quality index (QI) respectively.

The CQTI calculate as is show in Eq. 14 and it is the combination of three ballast layer indicators coming from the GPR which are the ballast depth exceedance (BDE), layer roughness index (LRI) and track drainage quality index (TDQI).

$$CTQI = LRI + 2 * BDE + TDQI \qquad \textit{Eq. 14}$$

Where:

LRI = layer roughness index. It indicates the degree of variance in the thickness in a layer over a given length. The LRI is designed to highlight areas where the thickness of the layer is changing rapidly. Such rapid variations can be an indication of sub-grade failure or wet bed formation.

BDE = ballast depth exceedance. Is the difference between the actual ballast layer thickness and the required ballast layer thickness. A minimum ballast thickness is required below the sleepers in order to provide correct support to the track and adequate drainage.

TDQI = track drainage quality index. This indicates the drainage adequacy of the ballast layer.

By means of the CTQI it is possible to classify the ballast layer condition in four different levels (being 1 the more severe and 4 good track conditions).

Similarly to the CTQI, the QI is also classified into four levels, with smaller numbers indicating a more serious defect of the track geometry. The QI refers to the ballast fouling index.

Finally, the QI2 reveals the railway line sections with track geometry deterioration that may or may not be related to the ballast layer conditions. The QI2 index is formulated as a rules matrix as is presented in Figure 35. This matrix ensures weighting when the track geometry is at severe level, which corresponds to the numbers “1” colored in black, indicating a very bad track condition. The other levels were represented by red, yellow and green (bad, moderate, good track conditions). Thanks to this QI2 matrix it is easier to identify those sections of track that require maintenance intervention.

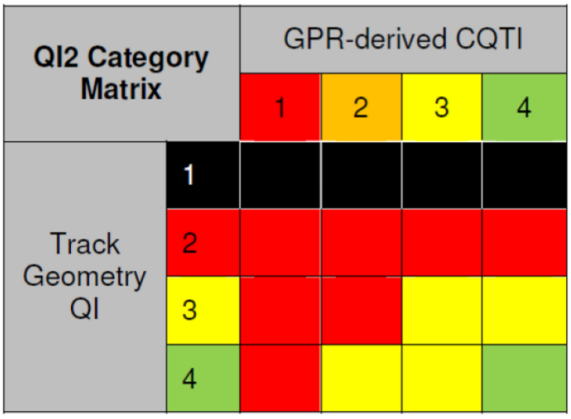

Figure 35. QI2 rules matrix between CQTI and track geometry QI (Eriksen, Gascoyne, & Fraser, 2011).

The results can be presented as a Work Order Recommendation (WOR). This indicates where and how to treat the trackbed, based on combining the GPR-derived metrics (layer and BFI) with the track geometry data (Eriksen, Gascoyne, & Fraser, 2011). The outputs of the WOR include summary tables that details the total length of each recommended maintenance type in the area studied, and also track charts which allow problem sections of track to be easily identified. An example is presented

in the Figure 36, from that can be easy identify those areas of the track which require maintenance intervention.

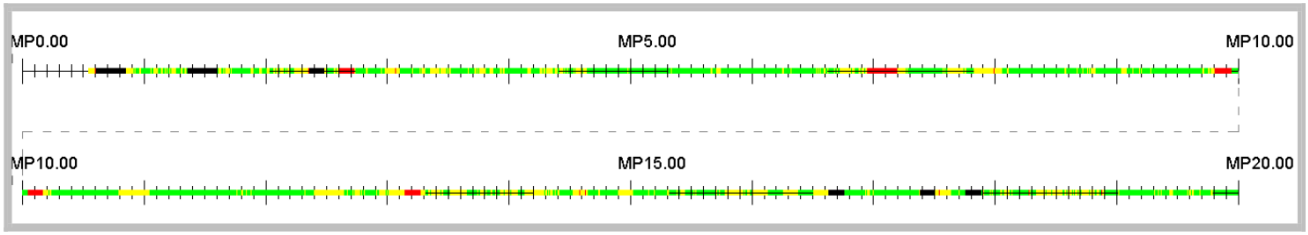

Figure 36. Track chart detailing QI2 result for 20 km section of track (Eriksen, Gascoyne, & Fraser, 2011).

2.5. GPR COMPARE WITH OTHER TECHNOLOGIES

As was mentioned at the beginning of this chapter, the GPR technology is not the only one capable to assess the ballast layer condition. However, the use of microwave systems is becoming popular all around the world in the health monitoring of railways (Manacorda & Simi, 2012).

The Table 11, propose by Wang et al. (2022), present the function of three monitoring equipment: GPR system, Track video and 3D laser scanning. Besides, in the third column each speed of operation is shown in order to compare those systems.

Equipment	Function	Maximum Operation Speed and Loading Platform
GPR system	Ballast layer thickness Ballast–subgrade interface Subgrade defects Mud-pumping Ballast fouling level Clean-fouled ballast interface Water content	160 km/h Railway comprehensive inspection trains, rail inspection vehicle, trolley
Track video (linear CCD camera)	Mud-pumping at surface Sleeper condition	160 km/h Railway comprehensive inspection trains, rail inspection vehicle
3D laser scanning	Ballast layer profile Surroundings Drainage	8 km/h Rail inspection vehicle, trolley

Table 11. Track inspection equipment system configuration, function, and recommended loading platform (Wang, et al., 2022).

It is evident that the GPR system turns out to be more complete in term of functions compared with the other equipment. GPR have the ability to determine ballast layer thickness, ballast-subgrade interface, subgrade defects, mud-pumping, ballast fouling levels, clean-fouled ballast interface and water content. An additional advantage of the GPR is that it provides a rapid measurement of substructure layer conditions with minimum interference to train operation

The main advantages of the GPR technology for the monitoring of railway substructure system were also expressed by Hyslip et al. (2005) and coincides with the one just presented above.

2.6. LIMITATIONS OF THE GPR IN BALLAST ASSESSMENT

Although the GPR is a complete tool for the assessment of the condition of the ballast, as was presented in the previous sections, the user must be aware of a few limitations with this technology.

Not detectable layers boundaries

According to Hyslip et al. (2005), one of the limitations of the GPR is that substructure layer boundaries may not be detectable when there is too little difference in electrical properties between the two adjoining layers. This can be illustrated in the study made by Al-Qadi, I., et al. (2008). They conduct a field GPR survey to evaluate the effectiveness of the technology to assess the railway ballast condition. The Figure 37 presents different fouling conditions in the ballast layer.

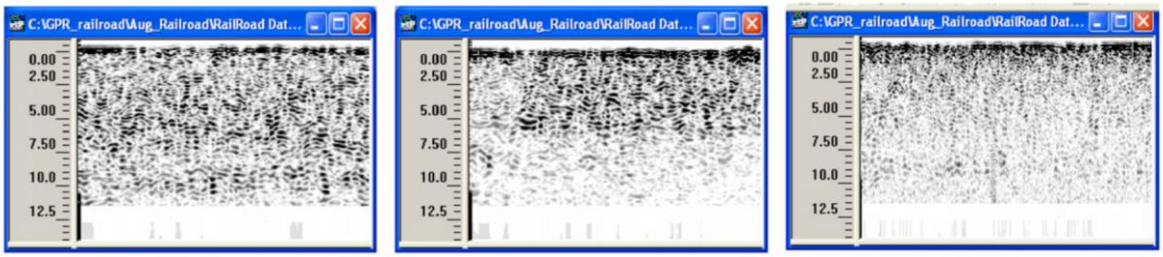

Figure 37. Ballast exhibition various fouling conditions (clean, moderately fouled and fouled ballast) (Al-Qadi, Xie, & Roberts, 2008).

It can be noticed that the clean ballast gave a more scattered response than fouled ballast, having a more regularly distributed scattering pattern. Then the second condition at the middle represents a moderately fouled condition where it is evident a variation in the scattering pattern for the bottom half of the image which is caused by changes in the size of air voids due to fouling. Thanks to that behavior, the boundary between clean and fouled ballast can be estimated. In the third case, the fouled ballast presents a weaker and shallower reflection of the electromagnetic waves therefore the boundary between clean and fouled ballast also becomes blurred.

As a conclusion from this study, as the ballast becomes progressively fouled, the reflection becomes less defined, and horizons become more difficult to track (Al-Qadi, Xie, & Roberts, 2008).

Another study case to reflect this limitation was presented before in the Figure 33 where the end of the ballast layer boundary (a deeper reflection) was not detected in the section C-D and D-E. A possible solution to that can be the installation of radar detectable geosynthetics during the construction of railways (Artagan, Bianchini Ciampoli, D'Amico, Calvi, & Tosti, 2019).

Not detectable boundaries can also occur due to the presence of high reflection materials that mask radar signals from lower layers. The conductivity of the material involved in the investigation controls the depth of penetration of the electromagnetic waves (Theodore & Sussmann, 1999). Therefore, highly conductive material significantly limits the penetration of the GPR wave. For example, metals materials are highly conductive and is considered a perfect reflector for GPR because no energy will penetrate. In general, soils that are highly conductive will not the suitable for investigation using GPR. The next table present a summary of the electromagnetic properties of some materials where it can be notice the remarkably high values of conductivity for the metal material and also for the wet soils.

Material type	**Dielectric constant**	**Velocity (m/ns)**	**Conductivity (s/m)**
Air	1	0.3	0
Metal	1-2	0.3-0.21	1x10^6
Wood	2.4-2.7	0.18-0.19	-
Concrete	4-10	0.15-0.095	-
Rock	4-10	0.15-0.095	0.01-0.00001
Asphalt	3-5	-	-
Water	80-81	0.034-0.033	0.003-0.0001
Granite (dry)	5	0.13	1x10^-8
Basalt (wet)	8	0.106	0.01
Granite (wet)	7	0.113	0.001
Sandy dry soil	2.6	0.186	0.00014
Sandy wet soil	25	0.06	0.0069
Clayey dry soil	2.4	0.194	0.00027
Clayey wet soil	15	0.077	0.05

Table 12. Soil dielectric constant, wave propagation velocity and conductivity. (Theodore & Sussmann, 1999)

Couple GPR data with track geometry information

Another limitation in the GPR is the fact that, only by reeling on the GPR data, the information is not enough to make maintenance decisions (Artagan, Bianchini Ciampoli, D'Amico, Calvi, & Tosti, 2019). It must be analyzed track geometry measurement along with the GPR data information in order to accurately prioritize problematic locations and also correctly assign maintenance resources.

Coupled with track geometry data, maintenance history, and other field testing, GPR provides insight on the location of changing subsurface conditions that is not easily obtained using another test (Theodore & Sussmann, 1999). It provides an efficient means of identifying those track geometry faults that are associated with an underlying measurable trackbed problem and helping determine the extent of that problem.

In the Figure 38 is presented a result of the combination of datasets where the first 2 charts are the ballast layer profile at the center and at the shoulders, the next one is a contoured map of depth to fouled ballast/formation. The following 3 charts are color strip type that shows the moisture index, thickness of ballast against defined thresholds, and ballast layer roughness (LRI). Then, 2D plots showing the ballast fouling index (BFI) at the left shoulder, center and right shoulder of the ballast formation are showed. The last 2 chart are color strip charts of the 1D BFI, and track geometry.

Finally, since geophysical testing requires test borings or excavations to calibrate the results to the site conditions, a combination of traditional testing and GPR can make investigations more efficient by limiting the number of traditional tests, while covering a larger percentage of the subsurface. If problems with the track substructure were identified, in-situ and laboratory testing would accompany the GPR testing to identify the root cause of the track problem. (Theodore & Sussmann, 1999).

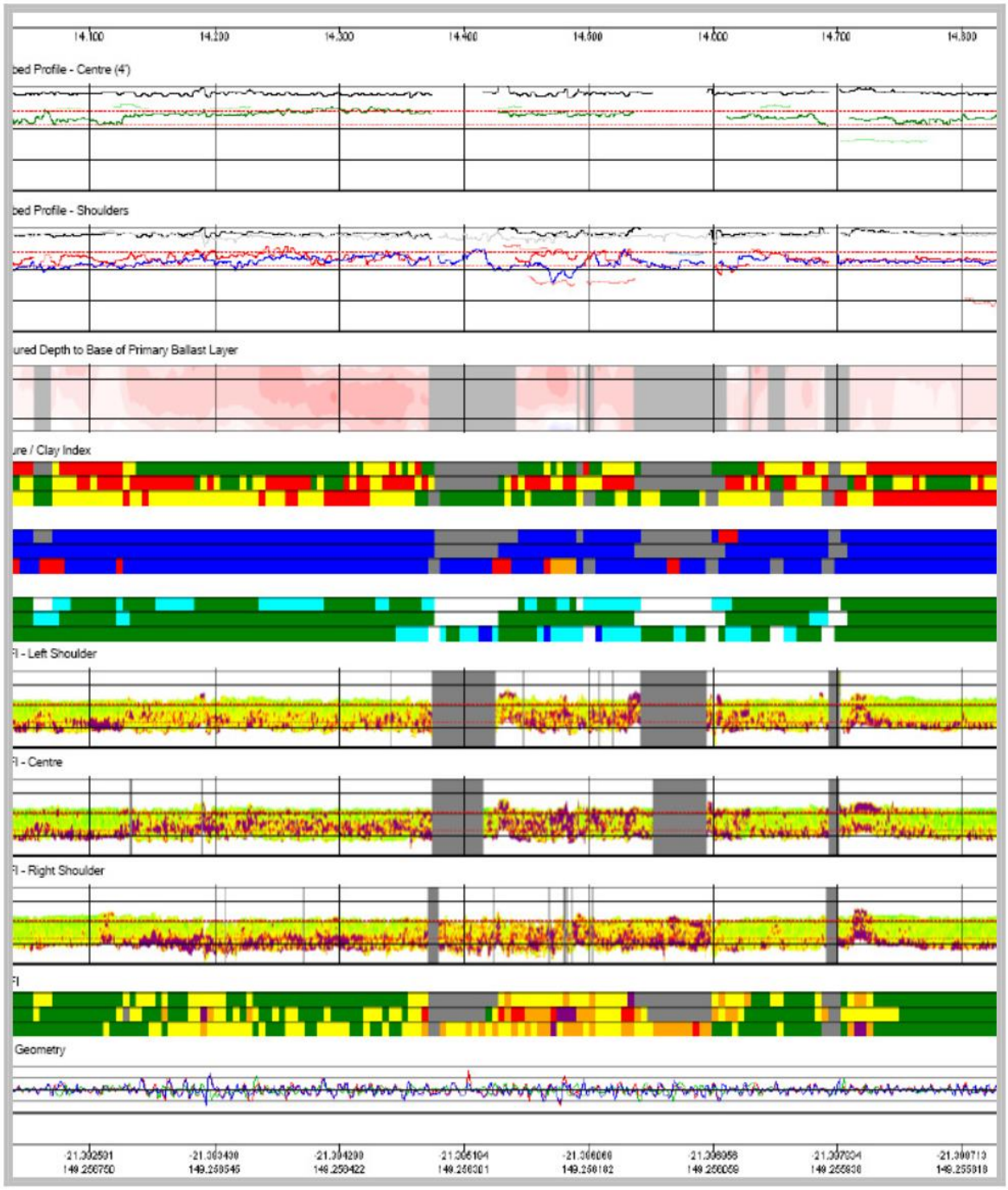

Figure 38. Report with data panels showing (top-bottom) – layers in the center, layers over the shoulders, a contoured map of depth to fouled ballast/formation, colour strip charts showing moisture index, thickness of ballast against defined thresholds, and ballast layer roughness, 2D BFI plots, colour strip charts of the 1D BFI, and track geometry (Top Up and Down + Twist). Linear meterage and GPS coordinates provided. (Eriksen, Gascoyne, & Fraser, 2011)

Noise in the signal

As a last limitation, there is the noise in the signal during the data collection process. According to Theodore & Sussmann (1999), noise can be of 2 types:

- Coherent: noise that can be predicted from location to location such as signal multiples
- Incoherent: random noise from either the system or surroundings

The formation of multiples in a signal occurs when materials that reflect significant energy (strong reflectors like rail and tie reinforcement) are encountered and the reflected energy reverberates in the subsurface (i.e., reflecting off multiple layers before detection by the receiver). The Figure 39 presents a path of multiples or ringing. Here the signal is transmitted form the antenna and then propagates into the subsurface. The reflector material reflects off the subsurface layer interface and a portion of the signal is reflected form the surface back into the subsurface, bounces off the layer interface again and is detected by the antenna.

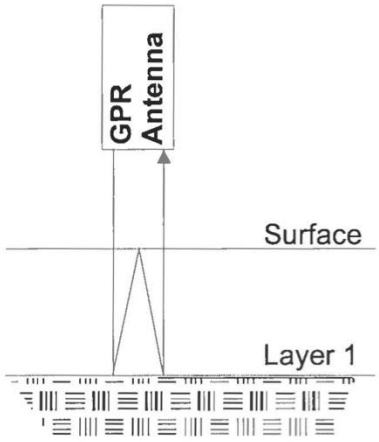

Figure 39. Formation of multiples or ringing (Theodore & Sussmann, 1999).

Even though the noise can be presence in the signal as false peaks (i.e., radar response caused by sources other than subsurface layer interfaces), it can be removed through data processing. In fact, after the data collection, additional efforts are needed to further improve the GPR data filtering and data analysis techniques (Leng & Al-Qadi, 2010). Signal processing refers to the process of modifying a signal to enhance desired components of it. The processing can be performed during data

collection or post processing. This can be done in terms of both time and frequency domain. Bianchini, C. et al. (2019) mention some of the processing procedures:

- Time-zero correction: for inspections conducted with an air-coupled antenna, direct wave arrival times (time-zero) are not horizontally aligned along the main longitudinal scanning direction. The air layer between the signal source and the surface is removed in order to set a common starting time for each trace.

- De-wow: typically, GPR sections show strong lower frequency harmonics which tend to distort the average amplitude of the GPR trace towards values different from zero. De-wow is a stationary low-pass filter that suppresses harmonics with a dominant frequency usually lower than a specific threshold.

- Background removal: Noise produces nearly perfect horizontal reflections that might mask actual reflections from real targets and produce unreliable results. To suppress background noise, like the signal ringing, the average GPR trace calculated using all the traces in the section is subtracted to every GPR trace, sample by sample.

- Band-pass filtering: Noise components are generally found to be outside the main working frequency bandwidth of a GPR system. The band-pass filtering works by cutting off these side bands from the collected spectrum.

- Short-time Fourier transform (STFT): the application of this method allows keeping data information in both time and frequency domain, by tracking the change of frequency spectrum with time (or depth).

CONCLUSIONS

Currently, the railway tracks with ballast are the main track type for all kinds of transportation. The ballast layer is the main component of those track and its principal function is to transmit the loading uniformly to the substructure, keep the sleepers in place and providing sufficient drainage. However, those function may be affected mainly by the fouling in the ballast layer which will cause a change in the original gradation of the material. In this order of ideas, frequent inspections and maintenance are required in the system. An early detection is imperative to took maintenance decisions at the right time and to reduce the risk of possible derailments.

This document present paper reports to create a state of art on the use of GPR technology for the assessment of railway ballast. From that was found that the fundamental soil properties influencing the GPR response are dielectric constant and conductivity. Those properties are strongly influence by the moisture contentment, therefore, the GPR is a suitable tool to localizing moisture changes in track. Additionally, it was described the electromagnetic characteristics of the ballast layer which it was found is highly depends on the material that is been inspected.

Within this investigation it is possible to conclude that the GPR, as a non-destructive technology for the assessment of the ballast, has the ability to detect most of the substructural problem as fouling content, poor layer thickness and composition of the subgrade layers, presences of water trap in the layer, subgrade failure or deformation, longitudinal variation of the layer conditions. Besides some limitations as is the not detectable boundaries and the noise in the signal.

Furthermore, using GPR to inspect the railway ballast layer has many advantages compared to other inspection techniques, such as non-contact, non-destructive to the ballast layer, fast inspection, and continuous measurement of the line rather than fixed point. GPR is a tool capable of generating a continuous image of the material under the tracks, with the capacity of performing surveys at a high speed.

To better perform the quantitative evaluation of the ballast layer, it is convenient to visualize the interrelationship of the track layout, GPR data, and the alignment and profile track geometry information. In this way it is possible to accurately identify track geometry problem location, relate the problem to track layout, and determine if it can be attributed to substructure degradation based on the GPR data.

Finally, by combining of traditional testing and GPR, the investigations are more efficient by limiting the number of boring excavation points while covering the larger percentage of the subsurface. The GPR has the potential to correctly find deteriorated track sections and reduce the total amount of drillings to a minimum since the part of the track that present variation will be punctually assessed and the boring point accurately located in representative part of the track. This will allow considerable cost savings in maintenance. Therefore, the use of a GPR can be considered to be a suitable and economic alternative compared to the other survey methods.

RECOMMENDATIONS

As one of the recommendations for future development of GPR for railroad application, it is the automatic data processing and interpretation. This should be included in order to provide a more automated assessment of track substructure. However this processing automation will requires standardization of the data acquisition process and therefore involves gaining experience by collecting data in a wide variety of field conditions.

Also, the GPR data together with track maintenance management software should be use together. The combination of those information will generally provide the best basis for evaluating track condition.

Moreover, the railway line type and the characteristics of the subgrade should be considered in order to carry out multi-scene data collection and calibration tests in different regional environments to establish a complete quantitative evaluation standard for the ballast layer condition and to guide the formulation of ballast layer maintenance strategies.

Finally, further investigation about the electrical properties of the track substructure material should be develop in order to get a better interpretation of the GPR data results.

BIBLIOGRAPHY

Bassey, D., Ngene, B., Akinwumi, I., Akplan, V., & Bamigboye, G. (2020). Ballast Contamination Mechanisms: A Criterial Review of Characterisation and Performance Indicators. *Infrastructures*.

Bianchini Ciampoli, L., Calvi, A., & D'Amico, F. (2019). Railway ballast monitoring by GPR: a test site investigation. *Remote Sensing*.

Hyslip, J., Olhoeft, G., Smith, S., & Selig, E. (2005). Ground penetrating radar for railroad track substructure evaluation . *U.S. Deparment of Transportation. Federal Railroad Administration. Officie of Research and Development.*, 48.

Silvast, M., Nurmikolu, A., Wiljanen, B., & Levomäki, M. (2013). Identifying frost-susceptible areas on Finnish railways using the ground penetrating radar technique. *Journal of Rail and Rapid Transit*.

Silvast, M., Nurmikolu, A., Wiljanen, B., & Levomaki, M. (2010). An inspection of railway ballast quality using ground penetrating radar in Finland. *Proceedings of the Institution of Mechanical Engineers, Part F: Journal of Rail and Rapid Transit*, 224(5), 345-351.

Li, D., Hyslip, J., Sussmann, T., & Chrismer, S. (2015). *Railways Geotechnics.* Taylor & Francis Group.

RailCorp. (2015, October). *Technical note – TN 061:2015, Withdrawal of ESC 240 Ballast and SPC 241 Ballast*. Tratto il giorno 2022 da Transport for NSW: www.asa.transport.nsw.gov.au

European norm EN 13450. (2002). Aggregates for railway ballast. European Standard.

Esveld, C. (1998). IMPROVED KNOWLEDGE OF CWR TRACK. *UIC/ERRI*, 8-9.

Rete Ferroviaria Italiana RFI . (2020). Parte II, sezione 17: Pietrisco per massicciata ferroviaria.

Jing, G., & Aela, P. (2020). Review of the lateral resistance of ballasted tracks. *Proceedings of the Institution of Mechanical Engineers, Part F: Journal of Rail and Rapid Transit*, 234(8), 807-820.

Guo, Y., Markine, V., & Jing, G. (2021). Review of ballast track tamping: Mechanism, challenges and solutions. *Construction and building materials*, 300, 123940.

Tutumluer, E., Huang, H., Hashash, Y., & Ghaboussi, J. (2009). AREMA gradations affecting ballast performance using discrete element modeling (DEM) approach. *In Proceedings of the AREMA 2009 annual conference* , (pp. 20-23).

AURIZON. (2015). Management of Ballast Fouling in the Central Queensland Coal Network. *A review of Ballast Management 2010 - 2017*.

Guidelines to the Best Practice for Heavy Haul Railway Operations. (2009). *International Heavy Haul Association Publication*.

AREMA. (2012). Manual for Railway Engineering. *American Railway Engineering and Maintenance of Way Association*.

Wang, S., Liu, G., Jing, G., Feng, Q., Liu, H., & Guo, Y. (2022). State-of-the-Art Review of Ground Penetrating Radar (GPR) Applications for Railway Ballast Inspection. *Sensors*, 22(7), 2450.

Benedetto, A., Tosti, F., Bianchini Ciampoli, L., Calvi, A., & Brancadoro, M. G. (2017). Railway ballast condition assessment using ground-penetrating radar – An experimental, numerical simulation and modelling development. *Construction and Building Materials*, 140, 508-520.

Al-Qadi, I., Xie, W., & Roberts, R. (2008). Scattering analysis of ground-penetrating radar data to quantify railroad ballast contamination. *NDT&E International*, 41(6), 441-447.

Saarenketo, T., & Scullion, T. (2000). Road evaluation with ground peneration radar. *Journal of Applied Geophysics*, 43(2-4), 119-138.

De Bold, R., O'Connor, G., Morrissey, J., & Forde, M. (2015). Benchmarking large scale GPR experiments on railway ballast. *Construction and Building Materials*, 92, 31-42.

Read, D., Meddah, A., Li, D., TTCI, & Mui, W. (2017). Ground penetrating radar technology evaluation on the high tonnage loop: phase 1.

Anbazhagan, P., Lijun, S., Buddhima, I., & Cholachat, R. (2011). Model track studies on fouled ballast using ground penetrating radar and multichannel analysis of surface wave. *Journal of Applied Geophysics*, 74(4), 175-184.

Barrett, B., Day, H., Gascoyne, J., & Eriksen, A. (2019). Understanding the capabilities of GPR for the measurement of ballast fouling conditions. *Journal of Applied Geophysics*, 169, 183-198.

Eriksen, A., Gascoyne, J., & Fraser, R. (2011). Ground penetrating radar as part of a holistic strategy for inspecting trackbed. *Australian Geomechanics Society*, 46(3), 1-11.

Gobel, C., Hellmann, R., & Petzold, H. (1994). Georadar-model and in-situ investigations for inspection of Railway Tracks. *Proceedings of the 5th International Conference on Ground Penetrating Radar*.

Theodore, R., & Sussmann, J. (1999). Application of Ground Penetration Radar to railway track substructure maintenance managment. *University of Massachusetts Amherst*.

Moaveni, M., Qian, Y., Boler, H., Mishra, D., & Tutumler, E. (2014). Investigation of Ballast Degradation and Fouling Trends using Image Analysis. *Railway Technology: Research, Development and Maintenance, J. Pombo, (Editor), Civil-Comp Press, Stirlingshire, Scotland.*, Vol. 123.

Artagan, S. S., Bianchini Ciampoli, L., D'Amico, F., Calvi, A., & Tosti, F. (2019). Non-destructive Assessment and Health Monitoring of Railway Infrastructures. *Surveys in Geophysics* , 41(3), 447-483.

The constructor. (2019, Marzo). Tratto da theconstructor.org: https://theconstructor.org/transportation/ballast-functions-types.

Lim, W. (2004). Mechanics of railway ballast behaviour. *The University of Nottingham*.

Calvi, A., Cutolo, E., Bianchini Ciampoli, L., & Brancadoro , M. (2016, May). *Ballast ferroviario: monitoraggio del degrado con georadar*. Tratto da Strade e autostrade: https://www.stradeeautostrade.it/materiali-e-inerti/ballast-ferroviario-monitoraggio-del-degrado-con-georadar/

Sadeghi, J., Motieyan-Najar, M., Zakeri, J., Yousefi, B., & Mollazadeh, M. (2018). Improvement of railway ballast maintenance approach, incorporating ballast geometry and fouling conditions. *Journal of Applied Geophysics*, 151, 263–273.

Selig, E., & Waters, J. (1994). *Track geotechnology and substructure management.* Thomas Telford.

Tennakoon, N., Indraratna, B., Rujikiatkamjorn, C., Nimbalkar, S., & & Neville, T. (2012). The role of ballast fouling characteristics on the drainage capacity of rail substructure.

ARTC, A. (2006). Track Drainage – Inspection and Maintenance. *Engineering Practices Manual Civil Engineering*, March.

ARTC, A. (2007). ETA-04-01: Ballast Specifications.

Benedetto, F., Tosti, F., & Alani, A. (2017). An entropy-based analysis of GPR data for the assessment of railway ballast conditions. *IEEE Transactions on Geoscience and Remote Sensing*, 55(7), 3900-3908.

Manacorda, G., & Simi, A. (2012). Non-Destructive Inspection and Characterization of Track Bed with Microwaves. *IEEE*, (pp. 805-810).

Daniels, D. (2004). *Ground Penetrating Radar. 2nd Edition.* London: IEE Radar, Sonar and Navigation Series 15 (Ed.).

Clark, M. R., Gillespie, R., Kemp, T., & McCann, D. M. (2001). Electromagnetic properties of railway ballast. *NDT & E International*, 34(5), 305-311.

Leng, Z., & Al-Qadi, I. (2010). Railroad ballast evaluation using ground-penetrating radar: laboratory investigation and field validation. *Transportation research record*, 2159(1), 110-117.

Manacorda, G., Morandi, D., Sarri, A., & Staccone, G. (2002). Customized GPR system for railroad track verification. *Ninth International Conference on Ground Penetrating Radar*, (Vol. 4758, pp. 719-723).

Zhang, Q., Eriksen, A., & Gascoyne, J. (2010). Rail radar-a fast maturing tool for monitoring trackbed. *Proceedings of the XIII Internarional Conference on Ground Penetrating Radar. IEEE.*, (pp. 1-5).

Vorster, D. J. (2012). The use of ground penetrating radar for track substructure characterization. *Masters of Engineering dissertation, University of Pretoria, Pretoria, South Africa*.

Tutumluer, E., & Huang, H. (2011). Discrete Element Modeling for fouled railroad ballast. *Construction and Building Materials*, 25(8), 3306-3312.

Selig, E. T., Parsons, B. K., & Cole, B. E. (1993). Drainage of railway ballast. *In Proceeding of the 5th International Heavy Haul Railway Conference"*.

Tutumluer, E., Huang, H., Hashash, Y., & Ghaboussi, J. (2006, September). Aggregate Shape Effects on Ballast Tamping and Railroad. *Proceedings of the AREMA Annual conference*, pp. 17-20.

Klassen, M. J., Clifton, A. W., & Watters, B. R. (1987). Track evaluation and ballast performance specifications . No. 1131.

Roberts, R., Al-Qadi, I. L., Tutumluer, E., & Kathage, A. (2007). Ballast fouling assessment using 2 GHz horn antennas-GPR and ground truth comparison from 238 km of track. *9th International Railway Engineering Conference*.